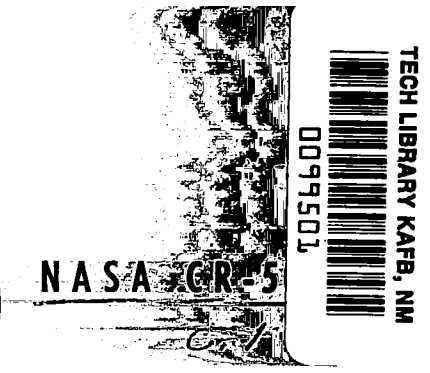

NASA CONTRACTOR REPORT

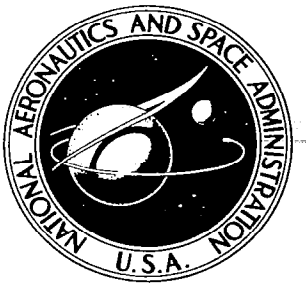

A WIND TUNNEL INVESTIGATION OF PANEL RESPONSE TO BOUNDARY LAYER PRESSURE FLUCTUATIONS AT MACH 1.4 AND MACH 3.5

by David Alan Bies

Prepared by
BOLT BERANEK AND NEWMAN, INC.
Van Nuys, Calif.
for

NATIONAL AERONAUTICS AND SPACE ADMINISTRATION • WASHINGTON, D. C. • MAY 1966

TABLE OF CONTENTS

A WIND TUNNEL INVESTIGATION OF PANEL RESPONSE TO BOUNDARY LAYER PRESSURE FLUCTUATIONS AT MACH 1.4 AND MACH 3.5

I. INTRODUCTION

With accelerating interest in the development of a supersonic transport, much time and effort have been devoted to the investigation of boundary layer turbulent pressure fluctuations, and to the response of structures to such a driving field. Interest in these investigations has also been strongly motivated by the need for quiet submarines, and for vibration control in missiles and reentry vehicles. This report describes a series of experiments investigating the structural response to boundary layer turbulence of a well-damped panel of high modal density. Investigations were conducted in the Douglas Aircraft Company 1' x 1' blowdown wind tunnel located in El Segundo, California

Two test panels were designed, constructed and tested. The panels were designed with two purposes in mind: 1) to obtain information about response which might be scaled to full-scale, and 2) to verify or reject the possible existence of surface Mach waves predicted by theory. The design of the experimental apparatus was also strongly influenced by the practical limitations of available materials and by special problems involved in the use of a blowdown wind tunnel. As a result of the above considerations, the test apparatus is unique, and it is discussed first in Section II below in some detail. Section III also contains further detailed description of the test apparatus. In Sections III and IV the results of wind tunnel testing and acoustic testing of the panels are reported. In Section V a comparison

and synthesis of some of the results of wind tunnel and acoustic tests is made. Some estimates of full-scale panel response are also made, and the results of experiments are compared with theoretical predictions based on material given in the Appendices. The summary and conclusions are given in Section VI.

The experiments discussed in this report represent an effort to develop a new approach to the problem of the interaction of boundary layer pressure fluctuations and structural response. They are exploratory in nature rather than final. The emphasis has been placed on the experimental aspects of the problem and not on the analytical approach, which has been carried out extensively elsewhere.

II. THE TEST PANELS

Consider for the moment a panel on the fuselage of a supersonic transport which is flying at about Mach 3 in the vicinity of 70,000 ft altitude. Such a panel will experience a pressure-fluctuation field over its surface due to the turbulent boundary layer. The overall sound pressure level of the pressure-fluctuation field might be of the order of 138 dB re .0002 microbar with a flat spectrum in the frequency range below 3 kcps (as measured by a microphone mounted flush with the exterior of the panel) that would roll off at the rate of 20 dB per decade above 3 kcps. (These estimates are discussed in Appendix A.) It might reasonably be assumed that a side-wall panel on a supersonic transport would be relatively large, and as a consequence, the modal density would be quite high above 100 cps. It is of interest to know how a panel of high modal density would respond to the expected boundary layer pressure fluctuation field. It is proposed that such information can be obtained with a suitable model panel, as described below.

A large body of information has been developed to describe the response of structures to pressure fluctuations. One theory (briefly outlined in Appendix B) has suggested the following interpretation. Below some upper frequency, called the coincidence frequency for any given panel and Mach number, the speed of propagation of the convected turbulent field across the surface of the panel will be greater than the speed of propagation of flexural waves in the panel. As a consequence, one might think of a convected turbulent eddy as producing a kind of bow wave in the panel which then propagates at some angle to the direction of propagation of the eddy. One might call such flexural waves "panel

Mach waves." The theory indicates that the direction of propagation of such panel Mach waves should be essentially normal to the direction of air flow for the frequency range well below the coincidence frequency for the panel. For the supersonic aircraft panel considered above, this is the frequency range of interest. The existence of panel Mach waves has been verified with the model panel described below.

The Douglas 1'x1' blowdown wind tunnel will operate at Mach 3.5, perhaps close enough to Mach 3 for testing purposes. At Mach 3.5 it has a boundary layer thickness of the order of 0.73 in. on the side wall in the test section. This dimension, if scaled by a factor of 5 for example, would correspond to the boundary layer thickness that one might observe on a supersonic transport at Mach 3.0 at 35 ft from a leading edge. (The latter estimate is discussed in Appendix A.) A scale factor of the order of 5 has been considered in constructing a model for testing.

Now we propose to depart from considerations of a directly scaled model and ask that our test panel be highly damped, perhaps much more so than a full scale panel might be on a supersonic transport. As shown in Appendix B, we may correct for loss of response due to high damping by scaling the resulting response in proportion to the reciprocal of the ratio of scale-model damping to full-scale damping. The purpose of the high damping in the model is to reduce the reverberant field in the panel, and thus to facilitate the identification of the driven field with its postulated panel Mach waves.

It would be advantageous to try to achieve an attenuation of flexural waves in the test panel of the order of 20 dB for a wave which starts near the center of the panel, travels

out to the edge, reflects, and returns back to the center. The size of the Douglas 1'x1' blowdown tunnel restricts the test panel to about 1' in diameter. We thus might seek an attenuation of the order of 20 dB/ft. In practice, much lower attenuation proved to be satisfactory.

The scaled frequency range is limited by two considerations. The interest in a high modal density imposes a lower limit on the frequency range, since it requires that the test panel be at least several wavelengths across. On the other hand, if we are to detect motion of the test panel by means of an accelerometer, the mass loading effect of the accelerometer will limit the upper frequency range. These considerations have restricted our model investigation to a frequency range from about 350 cps to 10,000 cps. On the basis of a scale factor of 5, this corresponds to a frequency range on a full-scale panel on a supersonic transport of 70 cps to 2000 cps.

We have briefly discussed our objectives and design criteria for the construction of model panels for test. The fabrication of the test panels proved to be much more difficult than anticipated, however. In addition, special problems associated with the use of a blowdown wind tunnel arose so that the models which were constructed and tested represent compromises. The desired high damping was not fully achieved, and the response of the panels was considerably complicated by the presence of a narrow backing cavity. (The narrow backing cavity was dictated by problems associated with the use of the blowdown wind tunnel.)

Two panels were constructed for response measurements. These consisted of either two .010" layers or two .005" layers of stainless steel sheet glued together with transfer adhesive

(Minnesota Mining and Manufacturing tape No. 465) .002" thick. Thus, the panels used for testing were nominally .022" and .012" thick respectively. The panels were rigidly fastened to retaining rings under slight tension to insure that they remained flat and would not "oil can" during use in the wind tunnel. The purpose of the sandwich construction was to provide a well-damped panel for response measurements. Some of the details of construction are shown in Fig. 1. Photographs of one of the panels and the associated retaining assembly are shown in Fig. 2.

The panels were tested in the Douglas 1'x1' blowdown wind tunnel whose construction and operation is described elsewhere.[1] The panel was mounted flush in the side wall of the tunnel. One of the panels is shown in Fig. 3 mounted in the side wall of the wind tunnel, where the wind tunnel side wall has been removed. The panel sandwich construction represents one of the compromises necessary to achieve high damping. The loss factors and wavelengths at various frequencies associated with flexural wave propagation in the test panels were separately investigated by testing sections typical of the sandwich construction. The results of these investigations are shown in Fig. 4. With the exception of the two points shown in the figure at 4 kcps and 8 kcps for the .012" thick panel, the loss factor and wavelength as a function of frequency for the two panels were determined by shaking a small cantilevered piece of the panel material and observing the root and tip motion.[2] The exceptions were estimated from measurements made directly on the plate. The plate was driven at its center and the displacement was determined at points spaced radially outward. In this frequency range the damping was sufficiently high that reflections at the edge were negligible. The difference between

observed response and that expected for a two-dimensional, radially expanding wave was used to estimate the damping.

The response of a panel to boundary layer or acoustic excitation was detected by means of two one-gram accelerometers attached to the back of the panel, the side opposite to the tunnel. The accelerometers were epoxied at positions on the panel on a 1" radius on opposite sides of the center of the panel. These details are shown in Fig. 1.

Some special problems associated with the use of a blowdown tunnel were considered in the construction of the panel response apparatus. These require some explanation. When the tunnel starts, a small overpressure proceeds down the tunnel, followed by a rapid decrease in static pressure to the equilibrium static pressure for the Mach number of the test condition. For example, the static pressure at Mach 3.5 is about 1.5 psi. When the tunnel stops, an overpressure proceeds back up the tunnel, and the static pressure then rapidly rises to atmospheric pressure.

The response of the panel during the start and stop phases of tunnel operation was quite violent and always resulted in breaking the epoxy bond between the accelerometers and the panel. Thus, it was necessary to clamp the panel during the start and stop phases of operation. This was accomplished by pumping the backing cavity on the back side of the panel down to a sufficiently low pressure that the static pressure in the tunnel would bottom the panel against the backing plate.

During the test phase of tunnel operation, between the start and stop phases, the backing cavity pressure was equalized

to the tunnel static pressure at the downstream edge of the panel. The requirements for rapid pressure equalization and panel clamping necessitated the use of a very shallow (.050" deep) backing cavity. As will be shown, the presence of the narrow backing cavity strongly influenced the response of the panel.

The response panel and its backing plate were in turn mounted on a retaining ring which mated to a circular orifice in the side wall of the wind tunnel. The mounting ring-panel assembly could be rotated on its mounting bolts so that the line of centers of the panel accelerometers could be placed at various angular orientations in thirty degree increments with respect to the direction of flow in the tunnel. Thus, the response of the panel along diameters parallel to the direction of flow, normal to the direction of flow, and at thirty and sixty degrees to the direction of flow could be investigated. Care was always taken to mount the panel flush with the interior wall of the wind tunnel.

In addition to investigating the response of the panels, it was also necessary to investigate the nature of the driving field. In the case of the Douglas 1'x1' tunnel this has been done previously.[1,3] It was convenient to associate these measurements of boundary layer pressure fluctuations with the measured response of the plate. It was thus of some interest to know that the presence of the panel did not sensibly perturb the boundary layer pressure fluctuation field. To check this possibility, a 1/4" Bruel and Kjaer microphone was flush-mounted on the downstream side of the mounting ring during several runs. The location of the microphone mounting hole is shown in Fig. 3. It was determined that the boundary layer pressure fluctuations were not sensibly affected by the presence of either panel.

III. WIND TUNNEL TESTS

A. Data Acquisition System

Figure 5 shows a schematic representation of the data acquisition system. Bruel and Kjaer sound level meters were used as decade amplifiers during recording. The acceleration spectra associated with the panel response were such that the overall levels observed at the time of recording agreed with the overall levels observed in playback of the recorded data. Thus, an accurate record was kept of the observed overall acceleration levels during each wind tunnel run. These recorded levels could then be used as a reliable and independent check on the system calibration during data playback and reduction. This facility proved very useful in ferreting out some instrumentation problems that occurred during the early part of testing.

The accelerometers used were Clevite type 2E3 one-gram accelerometers. These were chosen to minimize mass loading effects. Calculations indicated that the mass loading effect in the case of the thinner (.012") panel would only become important above 10 kcps. Thus all octave bands up to and including the 8 kcps octave band should be negligibly affected by mass loading. In mounting the accelerometers, care was taken to provide clearance around the accelerometers and around portions of their leads so that friction between the leads and the backing plate could also be neglected.

Acceleration data was recorded on two 54 kcps FM tracks at 60 ips on an Ampex tape recorder. The nominal upper data frequency cutoff was 10 kcps. Octave-band analysis of the recorded data might be as much as one decibel low in the 8 kcps octave band because of the 10 kcps cutoff frequency of the tape recorder. For the data considered here this possible error was considered negligible.

The phase response of the two tape channels used for recording was investigated before testing. A pair of record channels was chosen which had no more than five degrees inter-channel phase shift. End-to-end system calibration was provided by inserting a calibration voltage across a spare accelerometer substituted for the accelerometers mounted on the panel and recording the resulting signal. In addition, during the testing period when the accelerometers were removed from one panel and prior to epoxying them to the second panel, the accelerometers were calibrated at 100 cps on a General Radio accelerometer calibrator and the resulting signals were recorded, thus giving a true end-to-end calibration at this frequency. The results were found to be consistent.

Calibration of the 1/4" Bruel and Kjaer microphone used for pressure fluctuation measurements was provided at 250 cps by a Bruel and Kjaer pistonphone calibrator with a special adapter described elsewhere.[1/] The calibration tone and boundary layer pressure fluctuation signals were recorded sequentially on a direct-record channel and reduced on a Bruel and Kjaer octave-band analyzer immediately after each test.

B. Data Reduction System

The data reduction system is shown in Fig. 6. To facilitate data reduction, the original acceleration data in FM form was dubbed directly on a series of tape loops. The loops were then edited to remove portions of the signal recorded during the start and stop phase of tunnel operation when the plate was clamped. From eight to ten seconds of useful data were obtained. For octave-band spectra, the loops were played continuously and the output signal reduced by means of a Bruel and Kjaer sound level meter and octave band analyzer. As a check, one-third-octave-band spectra were obtained for a few runs and the results were found to be quite adequately described by the octave band analysis.

Correlation analysis made use of the same loops as described above. The analog correlator used for this purpose allowed investigation over the recorded frequency range up to ten kcps, and for delay times well in excess of those of interest for our purpose. The correlations were plotted directly on an x-y plotter. Only broad-band correlation was investigated.

C. Procedure Used for Response Measurements

The wind tunnel test procedure was as follows. Prior to tunnel start the pressure in the backing cavity was pumped down to about 0.5 psi. After tunnel start the pressure in the backing cavity was equalized to the tunnel static pressure at the downstream edge of the panel. About ten seconds of steady state data were recorded. Prior to tunnel shutdown the backing cavity pressure was again reduced to about 0.5 psi. When the tunnel

had been shut down the panel was rotated to a new position and the test was repeated. In this way measurements in thirty degree increments with respect to the direction of flow were made.

When the panel was installed or rotated in the tunnel wall, care was taken to maintain the panel surface flush with the interior wall surface of the tunnel. The panel was carefully shimmed for this purpose. However, some irregularities (as may be seen in Fig. 3) in the surface of the panel resulted from the method of attachment to the mounting ring. It was assumed that, if the measurement of boundary layer pressure fluctuations at the downstream edge of the panel gave results essentially the same as those obtained on a smooth flat plate, then the slight irregularities inherent in the edge structure of the panel were not of importance. As mentioned earlier, pressure fluctuation measurements with the panel in place were in agreement with earlier rigid flat plate measurements for unperturbed flow.

To be sure that the signals from the accelerometers were due to acceleration of the panel and not due to acoustic excitation in the small backing cavity, the accelerometers were placed unattached to the panel in the backing cavity and a wind tunnel test was run. Their response was of the order of 20 dB below that observed with the accelerometers attached to the panel. As a matter of fact, frequent opportunity was afforded to check this point during the early part of testing before the panel clamping scheme was developed for keeping the accelerometers attached to the panel.

The measurements of pressure fluctuations other than those mentioned above which are presented in this report were obtained during a separate series of tests. These measurements were obtained on a rigid plate. Based on the observation mentioned above that the results for unperturbed flow at the edge of the panel are the same as would be obtained on a flat plate, the assumption is made that the field at the center of the panel is the same as was measured on a rigid plate even for the cases of perturbed flow. The separate series of measurements is reported elsewhere by Douglas Aircraft Company,[3] and only that part of immediate interest for our purpose is repeated here.

D. Wind-Tunnel Experimental Results

Various test configurations which were investigated with the two panels are summarized in Table I. Unperturbed

TABLE I

FLOW CONFIGURATIONS TESTED IN PANEL RESPONSE INVESTIGATION

TEST CONFIGURATION	MACH NUMBER	
	test panel thickness .012"	test panel thickness .022"
Unperturbed flow	3.5, 1.4	3.5, 1.4
Thickened boundary layer	3.5	
Aft-facing step	3.5	3.5, 1.4
Mild shock	3.5	3.5
Expansion	3.5	3.5

flow refers to a fully developed turbulent boundary layer. The results of pressure fluctuation and vibration measurements for two panels at Mach numbers 3.5 and 1.4 for unperturbed flow are shown in Figs. 7 and 8. In these and in the subsequent figures angular positions of the accelerometers are measured with respect to the direction of air flow, with positive angles being up and negative angles being down.

A thickened boundary layer was produced by introducing surface roughness upstream of the panel. The roughness consisted of large-scale grit glued to the side wall. The resulting boundary layer was increased in thickness approximately eighty percent and was apparently fully developed. The flow was somewhat perturbed however by the presence of a small shock wave which resulted from the presence of grit and was reflected back on the upstream edge of the panel. The presence of this shock did not seem to affect the resulting panel response, however. The results of pressure fluctuation and vibration measurements with a thickened boundary layer are shown in Fig. 9. Comparison of this figure with Fig. 7a shows that the increase in pressure fluctuation level associated with the thicker boundary layer is accompanied by a corresponding increase in the vibration levels of the panel.

An aft-facing step consisting of a 3/4 inch thick insert extending from above the nozzle throat along the tunnel side wall to the upstream edge of the test panel was installed for some tests. Flow reattachment occurred within a couple of inches of the step at both Mach 3.5 and Mach 1.4, upstream of the point of attachment of the accelerometers to the panel. The results of measurements

with the step are shown in Figs. 10 and 11. Again comparison of these figures with Figs. 7 and 8 shows that a rise in pressure fluctuation levels is associated with a corresponding rise in vibration levels.

The mild shock and the expansion were generated by a generator installed in the center of the tunnel.[1,3] In the case of the mild shock and the expansion, the flow perturbations were centered on the panel. Thus, with the line of centers of the accelerometers parallel to the flow, the shock impinged on the plate between the accelerometers. When the line of centers of the accelerometers was normal to the flow, the shock impinged directly on their points of attachment. The results of these measurements are shown in Fig. 12 and Fig. 13. It may be noted that the panel response was less in the presence of a mild expansion than with unperturbed flow. This is in agreement with the generally lower boundary layer pressure fluctuations in the presence of a mild expansion.

In addition to the spectrum analysis of the panel response measurements, the cross correlation of the two accelerometers was investigated with a view to discovering the possible presence of panel Mach waves. With the panel dimensions, Mach numbers and frequency ranges chosen for this experiment panel, Mach waves should propagate in directions essentially normal to the direction of air flow across the plate. If the two accelerometers were placed so that they both saw the same panel Mach wave front at the same time, they would be correlated with zero time delay between them. If they were oriented in any other way, they would be much less correlated. Since the direction of wave-front propagation should be essentially normal

to the direction of flow, the accelerometers should show maximum correlation with zero time delay between them when their line of centers lay parallel to the air flow direction.

In Figs. 14 and 15 are shown the results of cross correlation for the .012" thick panel with unperturbed flow at Mach numbers 3.5 and 1.4. In each figure are shown four sets of curves based on measurements with the line of centers between the accelerometers parallel to the direction of flow, and at thirty degrees, at sixty degrees, and at ninety degrees to the direction of flow. The angle measured upward between the direction of flow and the line of centers of the accelerometers is designated in the figure as the roll angle. Positive delay in the figures corresponds to propagation of a disturbance parallel to the air flow, parallel and downward across the air flow, or downward across the air flow.

In Fig. 16 are shown the results of cross correlation of the accelerometer signals measured on the .022" thick panel at Mach 1.4. The results for roll angles of zero, thirty and sixty degrees are given. Failure of the test plate prevented a measurement of response at ninety degrees. Instrumentation problems encountered during the early part of testing prevented successful cross correlation of the accelerometer signals for the .022" thick panel at Mach 3.5. The data which is shown in Fig. 16 is, however, consistent with the prediction of decreasing correlation at zero time delay with increasing roll angle, if we suppose that the accelerometers were not quite lined up with the panel Mach wave fronts for the zero roll angle. This is possible since some difficulty was experienced with alignment during the early part of testing.

The Fourier transform of the cross correlation function should give the cross power spectral density function. By curve fitting an exponentially damped cosine curve to the correlation function for zero roll angle of Fig. 14, the cross power spectral density function was determined. It peaked at 1.1 kcps and had a shape in fairly good agreement with the spectrum shape indicated by the panel acceleration levels of Fig. 7.

It is tempting to try to infer more from the correlation data. For example, one might seek to associate propagation times with the displacement of correlation peaks. The reader is reminded that propagation of flexural waves is dispersive and this considerably complicates the interpretation of the cross correlation[4]. For this reason no attempt will be made to give further interpretation to the data of Figs. 14, 15, and 16.

IV. ACOUSTIC TESTS

A. Data Acquisition and Reduction System

The acoustic response of the test panels was investigated by immersing the panels in an acoustic field generated within a large bell jar. A number of rigid reflectors was installed within the bell jar to help promote a uniform reverberant acoustic field. The apparatus is schematically represented in Fig. 17. The figure shows that the bell jar could be evacuated so that the response of the test panel could be investigated at reduced pressures. The panels were exposed to octave bands of noise and their response in corresponding octave bands was determined.

B. Procedure Used for Response Measurements

In the acoustic tests the panel response was investigated for two configurations of the panel. In one case, the panel mounted on its backing plate (as shown in Fig. 1) was exposed to the sound field. In this case, one side of the panel was exposed to the sound field and the other side looked into the narrow backing cavity. The effect of the backing cavity at various static pressures was investigated. In the second case, the panel without the backing plate was mounted within the test chamber and both sides were exposed to the sound field. The two configurations were investigated several times each with slightly different configurations of the apparatus within the bell jar. Data typical of these tests are shown for the .012" thick panel without the backing plate at 7 psia static pressure in Fig. 18. The data of Fig. 18 are presented to give the reader an idea of the spread and levels encountered. The results of these measurements are discussed below.

V. DISCUSSION OF RESULTS

A. Comparison of Wind Tunnel and Acoustic Test Results

The data shown in Figs. 7 through 13 may be used to compute pressure fluctuation-to-acceleration transfer functions. As an example, transfer functions have been computed for the cases of unperturbed flow using the data shown in Figs. 7 and 8. The results are shown in Figs. 19 through 22.

A problem is raised by the pressure fluctuation data of Fig. 7a which becomes more severe in Fig. 8a. As reported previously[1] two sets of pressure fluctuation levels were observed on the Douglas 1'x1' wind tunnel sidewall. The lower set is in conformity with the generally accepted model of how boundary layer turbulent pressure fluctuations should behave. The upper set is anomalous and corresponds to perturbed flow. However, the work reported previously indicates that the higher levels are quite local and do not characterize the whole boundary layer. For this reason in computing transfer functions we have used pressure fluctuation levels which are the mean of the data points in the lower set in both Figs. 7a and 8a.

In Figs. 19, 20, and 21 we have plotted pressure-fluctuation-to-acceleration transfer functions for the .022" and the .012" thick panels based on measured response. In Fig. 22 we have plotted similar curves, although only the transfer function for the wind tunnel test is based directly on measurements. The other two curves in Fig. 22 are estimated from the data shown in the first three figures. The procedure for making these estimates is given below.

The wind tunnel transfer functions relate acceleration level in octave bands to boundary layer pressure fluctuation level in octave bands. They show the effectiveness of the turbulent boundary layer in driving the panel. The other two curves in Figs. 19-22 show the acoustic response of the panel with the backing plate in place (it is then structurally the same as it was when tested in the wind tunnel) and with the backing plate removed. In the latter case the measured acceleration response has been reduced 3 dB to account for the fact that in this case both sides of the panel were exposed to sound while in the other two cases the panel was exposed to a driving field on only one side.

We might give the following interpretation to the results shown in these figures. The backing cavity generally has negligible effect on the acoustic response of the panel in the high-frequency range of 4 and 8 kcps, but it greatly unloads the panel in the low-frequency range of 0.5, 1 and 2 kcps. The turbulent boundary layer pressure fluctuations are significantly more effective at high frequencies in driving the panel than is acoustic noise. In the low-frequency range of 0.5, 1 and 2 kcps for Mach 1.4, the two types of driving field are apparently equally effective. If there exists some low frequency below which such an equivalence might be observed for the Mach 3.5 data, it lies below the lowest frequency range of our data, i.e., below the 0.5 kcps octave band.

The procedure used in estimating the acoustic transfer functions shown in Fig. 22 is based on two assumptions which follow from the experimental results. It will be

shown in the following section that the assumption in Step 3 below is in essential agreement with the predictions of theory. The assumption in Step 2 below is also in agreement with theory which predicts that the response is pressure-insensitive. Since we wish to discuss the assumption in Step 3 in the following section, we choose to present the procedure for estimating the acoustic response curves shown in Fig. 22 here.

The following procedure was used in estimating the two curves shown in Fig. 22 for the acoustic-to-acceleration transfer functions.

1. We note by comparing Figs. 19 and 21 that the acceleration response for the .022" thick panel with the backing plate removed is essentially the same at 7 psi and 1.5 psi with the 1.5 psi response being generally higher by 1 or 2 dB.

2. We assume on the basis of Step 1 above that the same result would be true for the .012" thick panel. In Fig. 22 we have estimated the response for the .012" thick panel at 1.5 psi by adding 1 dB to the response shown in Fig. 20 for the same panel at 7 psi.

3. We note by reference to Fig. 21 that panel response to a boundary layer pressure fluctuation field is different from panel response to a reverberant acoustic field. We assume that the same quantitative differences would be observed for the .012" thick panel as were observed for the .022" thick

panel and use the differences shown in Fig. 21 to estimate the acoustic response shown in Fig. 22 from the wind tunnel test result. The assumption used here is fairly well corroborated by the data shown in Figs. 19 and 20. For example, if the data in Fig. 19 were used to estimate the acoustic test result shown in Fig. 20, the estimate and the experimental result shown in Fig. 20 would be in fair agreement.

B. Comparison of Theory and Experiment

1. Panel Response to Boundary Layer Pressure Fluctuations. For the panels considered in this report, the dominant component of acceleration in the frequency range of interest is due to hydrodynamic coincidence. Appendix B (B.18) gives for the component of acceleration due to hydrodynamic coincidence

$$Q_{HC}(\omega) = \frac{2\sqrt{3}\,\pi p_h^2 \cot\phi_c}{\rho^2 h^3 c_\ell\,\eta_{total}}\,\Phi_1(k_p\cos\phi_c)\,\Phi_3(k_p\sin\phi_c). \quad (1)$$

In this expression, Q_{HC} is the spectrum of the mean square acceleration. p_h is the root mean square overall pressure fluctuation. ρ and h are the density and thickness of the panel, and c_ℓ is the speed of propagation of plane longitudinal waves in the material of the panel. The panel loss factor is represented by η_{total}. k_p is the wavenumber associated with flexural waves propagating in the panel, and ϕ_c is the critical angle for flexural wave propagation. The functions Φ_1 and Φ_3 are the wavenumber spectra in the direction of air flow and normal to the direction of air flow, respectively.

The function $\mathcal{P}_1$ is given by (B.14) in Appendix B. With the understanding that $\mathcal{P}_1$ is the normalized spectrum of the convected pressure fluctuation field, we may use the data of Reference 1, Fig. 44c, to evaluate $\mathcal{P}_1$ as

$$\mathcal{P}_1 \approx 0.4 \frac{\tau^2}{p_h^2} \delta^* \frac{U_c}{U_\infty} \tag{2}$$

This approximation is shown as the dashed line in Fig. 7a. In this expression τ is the wall shear stress, δ^* is the boundary layer displacement thickness, U_c is the turbulent boundary layer convection velocity and U_∞ is the free stream air flow velocity.

In the evaluation of $\mathcal{P}_1$ given by (2), the simplification has been made that the pressure fluctuation spectrum is flat in the frequency range of interest. As seen by examining Fig. 7a, this is not strictly true. However, the approximation to the boundary layer pressure fluctuation level shown in the figure is considered to be good enough for our present purpose and in any case may easily be corrected by reference to the data shown in Fig. 7.

Appendix B gives as (B.21) the following expression

$$\mathcal{P}_3(k_p \sin \phi_c) = \frac{2\delta^*}{\pi[1 + (2\delta^* k_p \sin \phi_c)^2]} \tag{3}$$

for the wavenumber spectrum normal to the direction of flow. The expression defining the critical angle ϕ_c is given by (B.10) of Appendix B as

$$\cos \phi_c = \sqrt{\frac{\omega}{\omega_h}} \tag{4}$$

where ω_h is the frequency at which flexural wave propagation in the plate is equal to the convection velocity U_c of the turbulent boundary layer. The dimensions and frequency range of our panel response experiments have been chosen so that the critical angle is very nearly ninety degrees. If we use this information and (2), (3), and (4), we may transform (1) to read

$$\mathcal{A}_{HC}(\omega) = \frac{2\sqrt{3}\,\pi}{\rho^2 h^3 c_\ell\,\eta}\sqrt{\frac{\omega}{\omega_h}}\,\frac{0.8\tau^2\delta^{*2}U_c}{\pi U_\infty[1+(2\delta^* k_p)^2]} \quad . \tag{5}$$

It is convenient to put (3) in terms of directly measured observables and to convert spectrum level based on angular frequency to octave band level. Thus (5) becomes

$$\mathcal{A}_{\text{octave band}} = \frac{22.3\, f_c \tau^2 \delta^{*2}}{\lambda_p \rho_s^2 \eta U_\infty[1+(\frac{4\pi\delta^*}{\lambda_p})^2]} \tag{6}$$

where the flexural wavelength λ_p is given by

$$\lambda_p = \pi\sqrt{\frac{2c_\ell h}{\omega\sqrt{3}}} \tag{7}$$

In (6), f_c is the octave band center frequency and ρ_s is the panel surface density. In this form the equation applies equally well to a uniform panel or to a panel of sandwich construction such as considered in this report.

Equation (6) is expected to describe the panel response to boundary layer pressure fluctuations without the effect of a narrow backing cavity. We propose to correct our estimates of panel response by assuming that the effect of the backing cavity is the same for acoustic and boundary

layer pressure fluctuation excitation at the same static pressure. The pertinent data are given in Table II and the results of using (6) and correcting for cavity effect are summarized in Table III. The predicted responses are shown by the lines in Fig. 7. The agreement between the predicted and measured response for the two panels is quite encouraging.

2. Panel Response to Acoustic Excitation. The mean square acceleration response of a panel to a reverberant acoustic field of mean square pressure spectrum $S_a(\omega)$ is given in Appendix B, (B.6), as

$$\mathcal{Q}_a(\omega) = \frac{\sqrt{3}\,\pi c^2 \sigma}{\omega \rho^2 h^3 c_\ell\, \eta_{total}} S_a(\omega) \qquad (8)$$

If we use (7) above we may write (8) in terms of readily measured quantities as

$$\mathcal{Q}_a(\omega) = \frac{2\pi^3 c^2 \sigma S_a(\omega)}{\rho_s^2 \lambda_p^2\, \omega^2 \eta_{total}} \qquad (9)$$

We may write (9) as a transfer function as follows

$$\left(\begin{matrix}\text{Acceleration} \\ \text{level re 1 g}\end{matrix}\right) - \left(\begin{matrix}\text{pressure fluctuation} \\ \text{level re .0002 microbar}\end{matrix}\right) =$$

$$-134 + 10 \log \frac{2\pi^3 c^2 \sigma}{\rho_s^2 \lambda_p^2\, \omega^2 \eta_{total}} \qquad (10)$$

The radiation efficiency σ may be estimated using Reference 5. Following the reference we determine that for the .022" thick panel the radiation efficiency for sound incident on one side of the panel is

$$\sigma = 10^{-5} \sqrt{10f} \qquad (11)$$

TABLE II

PERTINENT DATA FOR CALCULATION PURPOSES
(Wind Tunnel Data from Reference 1)

Surface density of .022" panel	$\rho_s = .420$ gm/cm^2
Surface density of .012" panel	$\rho_s = .208$ gm/cm^2
Flexural wavelength of .022" panel	$\lambda_p = 135\ (\text{freq.})^{-1/2}$ cm
Flexural wavelength of .012" panel	$\lambda_p = 99\ (\text{freq.})^{-1/2}$ cm
Mach number	$M = 3.5$
Displacement thickness	$\delta^* = .778$ cm
Free stream velocity	$U_\infty = 6.47 \times 10^4$ cm/sec
Wall shear stress	$\tau = 9.12 \times 10^2$ dyne/cm^2
Speed of sound in tunnel	$c' = 1.87 \times 10^4$ cm/sec
Mean turbulent boundary layer convection velocity	$U_c = 5.25 \times 10^4$ cm/sec
Coincidence frequency for .022" panel	$\omega_h = 3\pi \times 10^5$ rad/sec
Coincidence frequency for .012" panel	$\omega_h = 6\pi \times 10^5$ rad/sec
Mach number	$M = 1.4$
Displacement thickness	$\delta^* = .173$ cm
Free stream velocity	$U_\infty = 4.03 \times 10^4$ cm/sec
Wall shear stress	$\tau = 14.6 \times 10^2$ dyne/cm^2
Speed of sound in tunnel	$c' = 2.96 \times 10^4$ cm/sec
Mean turbulent boundary layer convection velocity	$U_c = 3.22 \times 10^4$ cm/sec
Coincidence frequency for .022" panel	$\omega_h = 1.1\ \pi \times 10^5$ rad/sec
Coincidence frequency for .012" panel	$\omega_h = 2.2\ \pi \times 10^5$ rad/sec

TABLE III

CALCULATION OF TEST PANEL RESPONSE
BASED ON EQUATION (6)

Octave band center frequency f_c kcps	.5	1	2	4	8
.022" thick panel (surface density ρ_s = .420 gm/cm^2)					
loss factor η	.12	.077	.038	.023	.01
wavelength in plate λ_p(cm)	6.04	4.27	3.00	2.13	1.51
cavity correction dB	4	5	2	0	0
calculated response dB re 1 g using (6) and adding cavity correction	-3	2	4	6	11
.012" thick panel (surface density ρ_s = .208 gm/cm^2)					
loss factor η	.12	.09	.08	.07	.06
wavelength in plate λ_p(cm)	4.5	3.1	2.2	1.55	1.10
cavity correction dB	8	12	9	2	0
calculated response dB re 1 g using (6) and adding cavity correction	6	13	13	8	8

From the data given in Fig. 4 of the text we may determine the following empirical expression for the damping constant of the .022 " thick panel.

$$\eta = \frac{77}{f} \tag{12}$$

If we substitute (11), (12) and the expression for the flexural wavelength given in Table II into (10) and use the value for the surface density for the .022" panel (also given in Table II) we obtain

$$\left(\begin{matrix}\text{acceleration}\\ \text{level re 1 g}\end{matrix}\right) - \left(\begin{matrix}\text{pressure fluctuation}\\ \text{level re .0002 microbar}\end{matrix}\right) = -140 + 5 \log f \tag{13}$$

This equation may be compared with the data shown in Fig. 21 for the acoustic test with backing plate removed. The agreement with experiment in the 1 and 2 kcps octave bands is good, but the theoretical expression has a positive slope while the experimental data have a generally negative slope. Thus, the theoretical prediction diverges from the experimental values above and below the 1 and 2 kcps octave bands.

3. Ratio of Acoustic to Boundary Layer Pressure Fluctuation Excitation Efficiency. It is instructive to compare the acoustic and boundary layer pressure fluctuation excited acceleration response. After having put (5) in terms of the flexural wavelength by use of (7), divide (9) by (5) to obtain

$$\frac{a_a(\omega)}{a_{HC}(\omega)} = \frac{c^2 \sigma S_a(\omega)}{4\omega} \sqrt{\frac{\omega_h}{\omega}} \frac{\pi U_\infty [\,1 + (2k_p\delta^*)^2]}{0.4\tau^2\delta^{*2}U_c} \tag{14}$$

We let the acoustic spectrum be equal to the pressure fluctuation spectrum that would be measured in the turbulent boundary layer by a fixed microphone. Thus,

$$S_a(\omega) = \frac{p_h^2 \mathcal{P}_1}{U_c} \tag{15}$$

We substitute (2) into (15) and substitute the resulting equation into (14) to obtain

$$\frac{Q_a(\omega)}{Q_{HC}(\omega)} = \frac{c^2 \sigma \pi}{4\omega\delta^* U_c} \sqrt{\frac{\omega_h}{\omega}} \left[1 + (2k_p\delta^*)^2 \right] \tag{16}$$

Substitution of the numerical values given in Table II at Mach 3.5 into (16) shows that in the frequency range from .5 kcps to 8 kcps the acoustic response is less than the hydrodynamic coincidence response by 7 dB at the low frequency end to 8 dB at the high frequency end for the .022" thick panel, and by 6.5 dB over the whole range for .012". In Section V.A, it was assumed that the difference in response between boundary layer and acoustic excitation for the .012" thick panel would be the same as for the .022" thick panel. It may be seen that theory supports this assumption, since a difference in response of only one decibel is predicted by (16). In addition, the data of Fig. 21 are in general agreement with the result noted above.

According to (11), the radiation efficiency is proportional to the square root of the frequency, a result which is true for both panels. Reference to (16) shows that the frequency dependence of the quantity on the right side of the equation goes as a constant plus the reciprocal of the frequency. This is true because the panel wavenumber k_p is proportional

to the square root of the frequency. At Mach 3.5 the parameters are such that for both panels the frequency range of interest is near the asymptotic value of the function. The ratio of acoustic-to-hydrodynamic excitation is nearly constant for both panels. However, the situation at Mach 1.4 is quite different. In this case, the frequency range for both panels is in the region where the function changes rapidly. In this range according to (16), we should find acoustic excitation much greater than hydrodynamic excitation at low frequencies, while the opposite will be true at high frequencies. These trends are indicated in Figs. 19 and 20 by the experimental data.

The agreement noted above between theory and experiment is only qualitative, however. A sample calculation using the data given in Table II shows that (16) predicts equality between acoustic and hydrodynamic excitation at about 200 cps for the .022" thick panel, whereas equality is indicated experimentally at about 2 kcps.

4. Dependence of Panel Response on Thickness. It is of interest to know how the result discussed in the next section and shown in Fig. 23 compares with the prediction of theory. The responses for the two panels shown in the figure have been referenced to the same loss factor so that the two panels differ only in thickness. We shall consider how a change in panel thickness should affect panel response. The result of experiment indicated by the figure is that doubling the thickness reduces the panel response by about 2 dB at the low-frequency end and by about 4 dB at the high-frequency end. We shall see what behavior the theory predicts.

From (6) we obtain the following expression

$$\frac{Q_{HC12}}{Q_{HC22}} = \frac{\lambda_{p22}\rho_{s22}^2 \left[1 + 4\pi\delta^*/\lambda_{p22}\right]^2}{\lambda_{p12}\rho_{s12}^2 \left[1 + 4\pi\delta^*/\lambda_{p12}\right]^2} \tag{17}$$

Here the subscripts 12 and 22 have been added to distinquish parameters associated with the .012" thick panel and the .022" thick panel. Using the data in Table I and Fig. 4, we determine that the ratio defined by (17) ranges between eight at very low frequencies and two at very high frequencies for Mach 3.5. In the particular frequency range of interest, from .5 kcps to 8 kcps, the ratio ranges from 4.5 to 3.5, indicating that the response of the .022" panel should be about 6 dB lower than the response of the .012" panel. The agreement with experiment is only fair, perhaps because the curves shown in Fig. 23 are not directly the result of measurement but do contain some problematical manipulation.

C. Estimation of Panel Response for a Supersonic Transport

In order to estimate panel response to boundary layer turbulence for a supersonic transport, we assume that the transport panel response will be little affected in the frequency range of high modal density by a large static pressure differential across it, and that one side will be exposed to the turbulent boundary layer while the other side will look into a relatively large cavity. We may use the results shown in Figs. 19 through 22 to estimate response at the corresponding Mach numbers. To make these estimates, we assume that the effect of the backing cavity will be the same for the turbulence response as it is for the acoustic response. Thus, in the figures the wind tunnel test results should be

reduced by the difference in decibels between the acoustic response with and without backing of the test panel.

The estimates of panel response shown in Fig. 23 were obtained by operating on the data of Figs. 21 and 22 as follows:

1. The wind tunnel test results were reduced by the differences between the acoustic test results with and without the backing plate.

2. The resulting transfer functions were corrected for differences in damping between the test panels and some real airplane structure. The loss factors measured on a real airplane structure and shown in Fig. 4 were used as our model for a real structure. The mean-square response is inversely proportional to the loss factor as shown by (6).

3. The frequency scale was lowered by the assumed scale factor of five.

4. The expected supersonic boundary layer pressure fluctuation spectrum was taken to be 100 dB re .0002 microbar over the frequency range of interest, as discussed in Appendix A.

5. The estimated pressure fluctuation level of Step 4 and the resulting transfer function of Step 3 were used to estimate the expected vibration levels.

VI. SUMMARY AND CONCLUSION

Two test panels were designed and fabricated for the purpose of measuring panel response to boundary layer pressure fluctuations in the frequency range of high modal density. The response of these panels to a turbulent boundary layer under conditions of unperturbed and mildly perturbed flow at Mach 1.4 and Mach 3.5 was measured. In addition, the response of test panels to reverberant acoustic fields was also measured.

The following conclusions are drawn from the results of the experiment:

1. Fairly good quantitative agreement has been obtained between theoretically predicted and measured panel response to turbulent boundary layer pressure fluctuations for the cases of unperturbed flow. Correlation investigation of panel acceleration response yields results in qualitative agreement with theory, which predicts the existence of surface Mach waves.

2. To a fair approximation, one may associate a single transfer function with a panel which will relate acceleration response to turbulent boundary layer pressure fluctuations under conditions of unperturbed or mildly perturbed flow.

3. For the purpose of investigating response, the clamped panel may offer a better means of investigating the boundary layer pressure fluctuation field, especially

under conditions of mildly perturbed flow, than does a series of microphones, because the panel acts to smooth out local flow perturbations and give an average response and thus determines an average driving field.

4. At Mach 3.5 boundary layer pressure fluctuations were of the order of 6dB more effective in driving the .022" thick panel than comparable reverberant acoustic fields. This is in agreement with theory, which predicts the ratio to be 7 to 8dB.

5. At Mach 1.4 two regimes were observed. In the low-frequency range, a reverberant acoustic field was slightly more effective in driving the panels than were boundary layer pressure fluctuations. In the high-frequency range, the boundary layer pressure fluctuations were as much as 7 or 8dB more effective in driving the panel than the reverberant acoustic field. This observation is in qualitative agreement with the predictions of theory.

6. Theory predicts an increase in response to a reverberant acoustic field with increasing frequency. The opposite response was observed. However, the predicted and measured response curves cross in the mid frequency range of this investigation.

7. Model studies such as considered in this report may offer valid means for predicting full-scale response.

REFERENCES

1. J. S. Murphy, D. A. Bies, W. V. Speaker, and P. A. Franken, "Wind Tunnel Investigation of Turbulent Boundary Layer Noise as Related to Design Criteria for High Performance Vehicles, NASA TN D-2247, April 1964.

2. W. P. Rodden and S. Whittier, J. Acoust. Soc. Am. 34, 469 (April 1962).

3. W. V. Speaker and C. M. Ailman, "Spectra and Space-Time Correlations of the Fluctuating Pressures at a Wall Beneath a Supersonic Turbulent Boundary Layer Perturbed by Steps and Shock Waves," Douglas Aircraft Company report, (Oct. 1965), (submitted to NASA Oct. 1965).

4. E. F. Winter and D. A. Bies, J. Acoust. Soc. Am. 34, 472 (April 1962).

5. G. Maidanik, J. Acoust. Soc. Am. 34, 809 (June 1962), Fig. 5.

APPENDIX A

ESTIMATION OF BOUNDARY LAYER THICKNESS AND BOUNDARY LAYER PRESSURE FLUCTUATIONS TO BE ENCOUNTERED BY A SUPERSONIC TRANSPORT

We assume that the supersonic transport under consideration flies at an altitude of 70,000 ft in a standard atmosphere. We confine our attention to a flat panel in a region of unperturbed flow approximately 35 ft from a leading edge. We obtain the following table of values from our assumptions and ARDC standard atmosphere tables.[A.1]

kinematic coefficient of viscosity	2.12×10^{-3} ft^2/sec
velocity of sound, c	968 ft/sec
length from leading edge, ℓ	35 ft
Mach number, M	3
air density, ρ_a	1.40×10^{-4} slugs/ft^3
Reynolds number R	4.80×10^7

We use the well-known fifth power law[A.2] to calculate the boundary layer thickness δ

$$\frac{\delta}{\ell} = 0.37(R)^{-1/5}$$

and obtain $\delta = 4.5"$. At Mach 3 the ratio of the displacement thickness to the boundary layer thickness is approximately 0.37.[A.3] We use this value to obtain an estimate of the displacement thickness $\delta^* = 1.6"$. This value is approximately a factor of five larger than the displacement

thickness observed in the Douglas 1' x 1' tunnel at Mach 3.5 (see Table II of the text).

The generally accepted subsonic value for the ratio of overall mean square pressure fluctuations in a turbulent boundary layer to the free stream dynamic pressure is [A,4,A,5]

$$\frac{\sqrt{p_h^2}}{q} \approx 6\times10^{-3} \qquad (A.1)$$

The associated spectrum may be considered to be flat up to a frequency given by

$$\frac{\omega_o \delta^*}{Mc} \approx 1 \qquad (A.2)$$

after which the spectrum rolls off at a rate of the order of or greater than 20 dB per decade. Use of the estimates for displacement thickness, Mach number and velocity of sound given above and (A.2) leads to a value of 3.3 kcps for the roll off frequency.

This value and the assumption of a flat spectrum below 3.3 kcps allows us to estimate the expected boundary layer pressure fluctuation spectrum level. Using the values given above, we obtain for the free stream dynamic pressure $q = 2.81\times10^5$ dyne/cm^2. Use of (A.1) then gives 138 dB re .0002 microbar as the overall pressure fluctuation level. Using our assumption of a flat spectrum below 3.3 kcps that rolls off quite abruptly above 3.3 kcps, we may compute the value of the constant spectrum level.

We take the spectrum bandwidth as 3.3 kcps and determine the spectrum level to be approximately 103 dB re .0002 microbar.

There is some evidence[A.5] which indicates that the constant in (A.1) may diminish and the constant in (A.2) may increase as the Mach number increases supersonically. The reference cited indicates that the constants may be of the order of 2×10^{-3} and 3, respectively, at Mach 3.0. If these values are used, the spectrum roll off frequency becomes 9.9 kcps and the overall sound pressure level becomes 128 dB. The corresponding spectrum level in this case is approximately 88 dB re .0002 microbar.

The difference between the two estimates of spectrum level is 15 dB. As a compromise we shall calculate panel response as shown in Fig. 23 of the text using a spectrum level of 100 dB re .0002 microbar. When the matter of spectrum level has been resolved, the data in Fig. 23 may be suitably corrected.

REFERENCES FOR APPENDIX A

A.1 The ARDC Model Atmosphere, 1959, AFCRC-TR-59-267.

A.2 H. Schlichting, Boundary Layer Theory (Pergamon Press, New York, 1955).

A.3 D. A. Bies, "A. Brief Investigation of Flight and Wind Tunnel Measurements of Boundary Layer Pressure Fluctuations," Part II of the second quarterly progress report, NASA Contract NASw-932, November 1964.

A.4 J. S. Murphy, D. A. Bies, W. V. Speaker, and P. A. Franken, "Wind Tunnel Investigation of Turbulent Boundary Layer Noise as Related to Design Criteria for High Performance Vehicles," NASA TN D-2247, April 1964.

A.5 W. V. Speaker and C. M. Ailman, "Spectra and Space-Time Correlations of the Fluctuating Pressures at a Wall Beneath a Supersonic Turbulent Boundary Layer Perturbed by Steps and Shock Waves," Douglas Aircraft Company report, October 1965 (submitted to NASA, October 1965).

APPENDIX B

THEORETICAL CONSIDERATIONS

Various reports and papers have presented calculations of the response of a thin elastic plate to sound fields and to convected, decaying pressure fields representative of the induced wall pressure of boundary layer turbulence. This appendix summarizes those results that are most pertinent to the interpretation of the panel response experiments.

The first part of this appendix summarizes the results relating to panel response to an acoustic field, and the second part summarizes the results relating to panel response to a turbulent boundary layer. In each of these two parts, we present the results first for free (resonant) response and then for forced (nonresonant) response. We also include some results related to the reradiation of sound by the vibrating panel. Although these results are not directly applicable to the panel response experiments performed on this program, they are illustrative of the general approach involved in considering sound reradiation to internal spaces.

A. Acoustic Response

Consider a statistically homogeneous sound field, with a pressure spectrum $S_a(\omega)$ measured at some position removed from walls or scatterers. (On a rigid wall large compared to a sound wavelength, "pressure doubling" of nongrazing waves will occur when the field is isotropic, and this effect

produces a spectral density $2S_a(\omega)$ on the wall.) On a thin flexible panel immersed in this sound field, the mechanical power input spectral density II_a to the panel is given by [B.1]

$$II_a = \frac{2\pi^2 c^2}{\omega^2 \rho h} \sigma n_s S_a(\omega) \langle D \rangle \tag{B.1}$$

where c is the speed of sound in the fluid, ω is the circular frequency, ρ is the density of the panel, h is the total thickness of the panel, n_s is the modal density of the panel, σ is the radiation effeciency of the panel, and $\langle D \rangle$ is an average directivity factor. We will assume that the sound field is isotropic, and $\langle D \rangle$ is therefore unity. For a flat plate, [B.2] the modal density

$$n_s = \frac{A}{4\pi k c_\ell} \tag{B.2}$$

where A is the area of the panel, k is the radius of gyration of the panel cross-section, and c_ℓ is the longitudinal wave speed of the panel material. For a homogeneous panel, the radius of gyration

$$k = \frac{h}{2\sqrt{3}} \tag{B.3}$$

The radiation effeciency σ of supported panels has been calculated by Maidanik [B.3] when one side of the panel is exposed to the sound field. When both sides of the panel are exposed to the sound field, his values of radiation effeciency should be doubled. The expression for σ

appropriate for the wind tunnel test panel exposed on one side to sound is presented in Reference B.3 in terms of the panel dimensions and ω_c, the acoustic critical frequency, the frequency at which the speed of sound in the surrounding fluid is equal to the speed of sound on the panel.

The resonant velocity response spectrum $\mathcal{V}(\omega)$ is found from the resonant input power by requiring that the dissipated power equal that absorbed from the sound field, or

$$\mathcal{V}_a(\omega) = \frac{II_a}{\omega\rho h A \eta_{total}} \tag{B.4}$$

where η_{tot} is the total panel damping. Combining (B.1), (B.2), (B.3), and B.4) with the expression for acceleration spectrum $\mathcal{A}(\omega)$

$$\mathcal{A}(\omega) = \omega^2 \mathcal{V}(\omega) \tag{B.5}$$

we obtain

$$\boxed{\mathcal{A}_a(\omega) = \frac{\sqrt{3\pi}\, c^2}{\omega\rho^2 h^3 c_\ell\, \eta_{total}}\, \sigma\, S_a(\omega)} \tag{B.6}$$

The nonresonant (forced) "mass law" acceleration spectrum of a panel above its first mode is given by (one side exposed)

$$\boxed{\mathcal{A}(\omega) = S_a(\omega)\, \frac{2}{\rho^2 h^2}} \tag{B.7}$$

B. Turbulence Response

Several models of the turbulent boundary layer pressure field have been proposed. We use the convected and decaying correlation pattern proposed by Ffowcs Williams and Lyon.[B.4] The pressure correlation has the form [B.5]

$$\mathcal{P}(\vec{\lambda},t) = \mathcal{P}_x(\lambda_1 - U_c t, \lambda_3)\, \mathcal{P}_t(\tau) \qquad (B.8)$$

with a Fourier-transformed power spectrum

$$\mathcal{P}(\vec{k},\omega) = \mathcal{P}_x(\vec{k})\, \mathcal{P}_t(\omega - k_1 U_c) \qquad (B.9)$$

where U_c is the convection speed, and k_1 and k_3 are the wavenumber components conjugate to the spatial separation variables λ_1 and λ_3. The direction of convection is λ_1.

The frequency $\omega_h = U_c^2 / kc_\ell$ is called the hydrodynamic critical frequency. For high-speed aircraft, the frequency range below the hydrodynamic critical frequency ($\omega < \omega_h$) is generally of primary interest. In this frequency range, the most strongly excited modes are the "hydrodynamically-coincident" (HC) modes. These modes propagate at an angle ϕ_c to the direction of propagation, where

$$\cos \phi_c = \sqrt{\frac{\omega}{\omega_h}} \qquad (B.10)$$

The mechanical power input spectral density for HC modes is given by [B.5]

$$II_{HC} = 8\pi p_h^2 G_\infty A \frac{\cot \phi_c}{\omega} \mathcal{P}_1(k_p \cos \phi_c) \mathcal{P}_3(k_p \sin \phi_c) \quad (B.11)$$

where we have assumed that the wavenumber spectrum is separable into downstream ($\mathcal{P}_1$) and cross-stream ($\mathcal{P}_3$) factors. p_h is the overall rms turbulent boundary layer pressure. G_∞ is the infinite plate input conductance, given by

$$G_\infty = \frac{1}{8\rho h \kappa c_\ell} \quad (B.12)$$

k_p is the wavenumber for free bending waves on the plate, given by

$$k_p = \sqrt{\frac{\omega}{\kappa c_\ell}} \quad (B.13)$$

The downstream wavenumber spectrum $\mathcal{P}_1$, may be evaluated in terms of the measured fixed-point pressure spectrum $\mathcal{P}_M$

$$\mathcal{P}_1(k_p \cos \phi_c) = \mathcal{P}_M(\frac{\omega}{U_c}) = U_c \mathcal{P}_M(\omega) \quad (B.14)$$

This relationship is based on the hypothesis that the measured spectrum results essentially from the convection in the x_1- direction of the eddy pattern over the fixed microphone.

For $\omega < \omega_h$, there is power input to "hydrodynamically-fast" (HF), "hydrodynamically-slow" (HS), and HC modes. A measure of the power input to the HF and HS modes is given by

$$II_{HF} = p_h^2 \, G_\infty A_t(k_p \delta^*) \, \Phi_t(\omega) \, A \qquad (B.15)$$

where A_t is an effective "correlation area," defined as an average of the wavenumber spectrum.[B.4] A simple form that is frequently assumed for the spectrum function Φ_t is

$$\Phi_t(\omega) = \frac{2\theta}{\pi} \frac{1}{1 + \omega^2\theta^2} \qquad (B.16)$$

where θ is the mean eddy lifetime, related to the convection speed U_c and displacement boundary layer thickness δ^* by the experimentally determined expression

$$\theta \approx 25 \frac{\delta^*}{U_c} \qquad (B.17)$$

For $\omega > \omega_h$, only HF modes can be excited, and (B.15) can be used directly to give the resonant response.

The various expressions for input power spectra may be converted to acceleration spectra by the use of (B.4) and (B.5). Thus, for HC modes,

$$Q_{HC}(\omega) = \frac{2\sqrt{3}\,\pi}{\rho^2 h^3 c_\ell \eta_{total}} p_h^2 \cot \phi_c \, \Phi_1(k_p \cos \phi_c) \, \Phi_3(k_p \sin \phi_c) \qquad (B.18)$$

and, for HF modes,

$$Q_{HF}(\omega) = \frac{\sqrt{3}\,\omega}{4\rho^2 h^3 c_\ell \eta_{total}} p_h^2 \, A_t(k_p \delta^*) \, \Phi_t(\omega) \qquad (B.19)$$

In addition to the HS, HC, and HF modes of resonant response, there is also a nonresonant (forced) response to turbulent boundary layer pressure fluctuations. A major part of this nonresonant response arises from excitation by wavenumbers smaller than k_p, the wavenumber for free bending waves on the plate. The response in this region depends only on the surface density of the structure and is referred to as "mass-controlled." This response is somewhat analogous to the "mass-law" response of a panel to acoustic excitation. For $\omega < \omega_h$, Lyon [B.6] has shown that the nonresonant acceleration spectrum is given by

$$\mathcal{Q}(\omega) = \frac{2p_h^2}{\pi\rho^2 h^2 U_c} \Phi_1(k_p \cos\phi_c) \arctan(2k_p\delta^* \sin\phi_c), \quad \omega < \omega_h \tag{B.20}$$

where the spectrum suggested by Hodgson's correlation data [B.4] has been used to evaluate the cross-stream wavenumber spectrum

$$\Phi_3(k_3) = \frac{2\delta^*}{\pi[1 + (2k_3\delta^*)^2]} \tag{B.21}$$

The ratio of forced to free response for $\omega < \omega_h$ is then found by comparing (B.20) with (B.18).

An additional complication enters if we are interested in reradiated sound rather than structural response, since wavenumbers less than the acoustic wavenumber k_o radiate sound considerably better than wavenumbers greater than k_o. The acceleration spectrum corresponding to the good-radiation range is obtained from (B.20), with k_p replaced by k_o.

$$\mathcal{A}(\omega) = \frac{2p_h^2}{\pi\rho^2 h^2 U_c} \mathcal{P}_1(k_o \cos\phi_c) \arctan(2 k_o \delta^* \sin\phi_c), \quad \omega < \omega_h \tag{B.22}$$

The ratio of forced to free radiation for $\omega < \omega_h$ is found by comparing a velocity spectrum based on (A.21) (with ρc loading) with one based on (B.18) (with a radiation loss factor η_{rad}).

For $\omega > \omega_h$, Lyon [B.6] has shown that the nonresonant acceleration spectrum is given by

$$\mathcal{A}_{HF}(\omega) = \frac{\pi k_p^2}{\rho^2 h^2} A_t p_h^2 \mathcal{P}_t(\omega) \tag{B.23}$$

where it has been assumed that the wavenumber spectrum is constant at low numbers, in agreement with considerable experimental data. The ratio of nonresonant to resonant response for $\omega > \omega_h$ is then found by comparing (B.23) with (B.19).

REFERENCES FOR APPENDIX B

B. 1 P. W. Smith and R. H. Lyon, "Sound and Structural Vibration," NASA CR-160, March 1965, Eq. (V.7.4).

B.2 ibid, Eq. (IV.5.19).

B.3 G. Maidanik, "Response of Ribbed Panels to Reverberant Acoustic Fields," J. Acoust. Soc. Am. 34, 809 (1962).

B.4 J. E. Ffowcs Williams and R. H. Lyon, "The Sound Radiated from Turbulent Flows near Flexible Boundaries," BBN Report No. 1054, August 1963 (to be published as an Agardograph).

B.5 R. H. Lyon, "Boundary Layer Noise Response Simulation with a Sound Field," Second International Conference on Acoustical Fatigue, Dayton, Ohio, April 1964.

B.6 R. H. Lyon, BBN internal memorandum, July 1965.

APPENDIX C

LIST OF SYMBOLS

A	area of panel
A_t	effective correlation area
$\mathcal{Q}(\omega)$	acceleration spectrum
$\mathcal{Q}_a(\omega)$	spectrum of the mean square acceleration due to acoustic excitation
$\mathcal{Q}_{HC}(\omega)$	spectrum of the mean square acceleration due to hydrodynamic coincident mode excitation
$\mathcal{Q}_{HF}(\omega)$	spectrum of the mean square acceleration due to hydrodynamically fast mode excitation
$\mathcal{Q}_{\text{octave band}}$	mean square octave band acceleration
c	speed of sound in air at normal temperatures
c'	speed of sound in tunnel at reduced temperatures
c_ℓ	speed of longitudinal waves in material of panel
$\langle D \rangle$	average directivity index
f	frequency
f_c	octave band center frequency
G_∞	infinite plate input conductance
h	thickness of a uniform panel
$\vec{k}$	vector wavenumber describing the turbulent boundary layer
k_p	wavenumber associated with flexural wave propagation
k_1, k_3	wavenumber component parallel to flow and normal to flow

k_o	acoustic wavenumber
ℓ	length from leading edge
M	Mach number
n_s	modal density of the panel
p_h	root mean square overall pressure fluctuation
Φ	pressure correlation function
Φ_1, Φ_3	wavenumber spectrum in direction of flow, and normal to flow and parallel to wall respectively
Φ_M	fixed-point pressure spectrum
Φ_t	temporal part of the pressure correlation function
Φ_x	spatial part of the pressure correlation function
q	free stream dynamic pressure
R	Reynolds number based on length
$S_a(\omega)$	acoustic pressure spectrum
t	time delay
U_c	mean convection velocity of turbulent boundary layer
U_∞	free stream air flow velocity
$\overline{v^2}$	mean square velocity spectrum
$\overline{v_a^2}$	mean square velocity spectrum response to acoustic excitation
δ	boundary layer thickness
δ^*	boundary layer displacement thickness
η	loss factor (defined as complex part of Young's modulus)

η_{total}	total loss factor including radiation loss as well as losses in medium
θ	mean eddy lifetime
κ	radius of gyration of a panel of uniform material
$\vec{\lambda}$	directed flexural wavelength in panel (vector)
λ_1, λ_3	components of flexural wavelength parallel to flow, normal to flow
λ_p	flexural wavelength in panel
II_a	mechanical power input spectral density function for acoustic excitation
II_{HC}	mechanical power input spectral density function for hydrodynamically coincident modes
II_{HF}	mechanical power input spectral density function for hydrodynamically fast modes
ρ	density of uniform panel material
ρ_a	density of air
ρ_s	surface density of panel
σ	radiation efficiency
τ	wall shear stress (skin friction)
ϕ_c	critical angle of panel Mach wave propagation
ω	angular frequency
ω_h	angular frequency at which flexural wave velocity equals mean turbulent boundary layer convection velocity

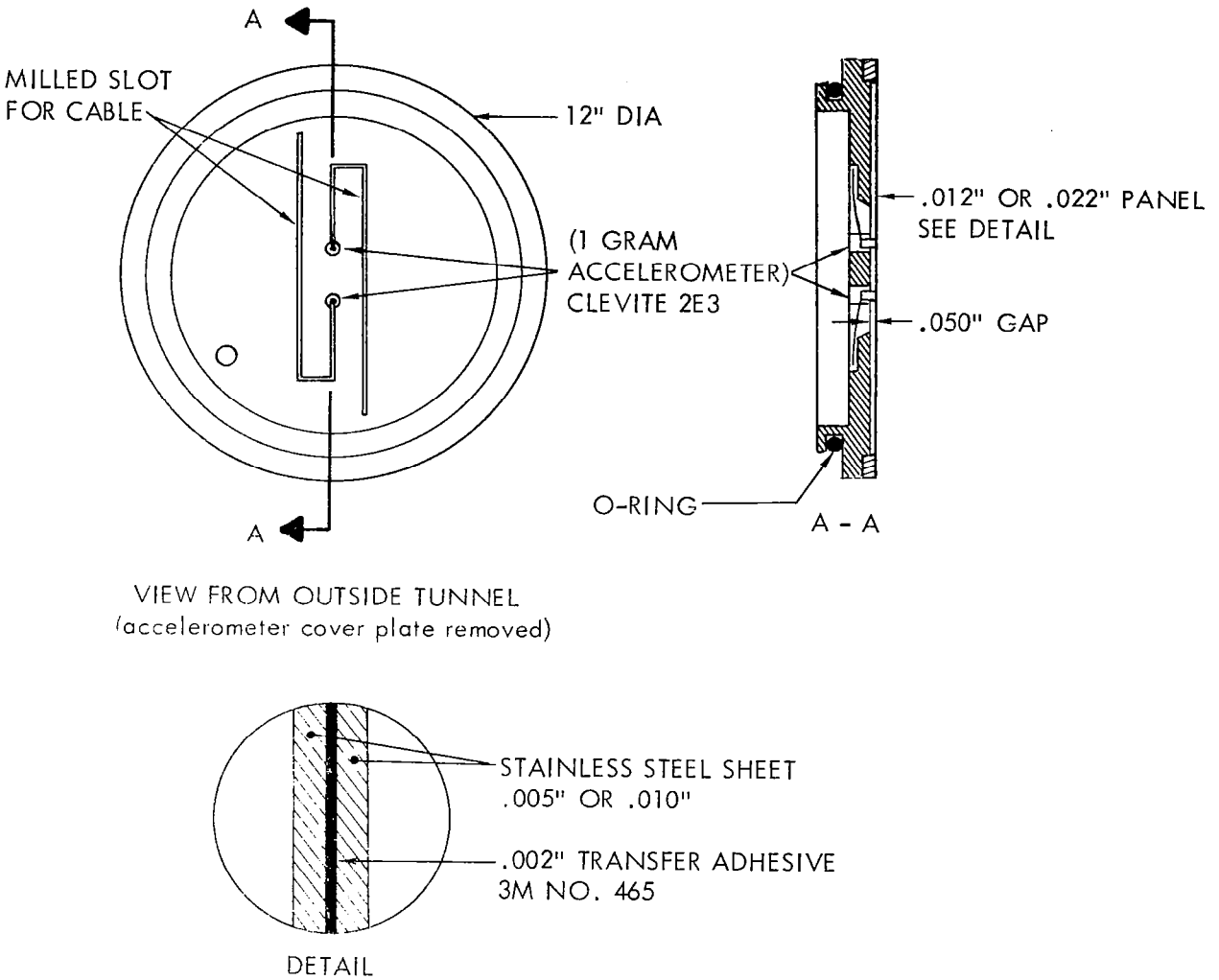

FIGURE 1. MODEL FOR TESTING PANEL RESPONSE TO BOUNDARY LAYER PRESSURE FLUCTUATIONS

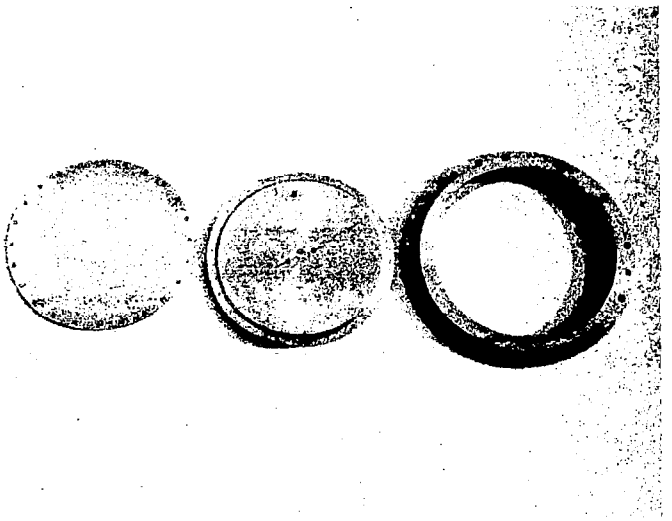

Front View Showing Test Panel,
Backing Plate and Retaining Ring

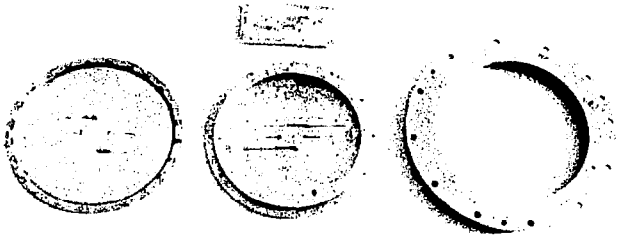

Back View Showing Test Panel with
Accelerometers Attached, Backing Plate,
Cover Plate, and Retaining Ring

FIGURE 2. TEST PANEL ASSEMBLY

FIGURE 3. TEST PANEL INSTALLED IN WIND TUNNEL SIDE WALL

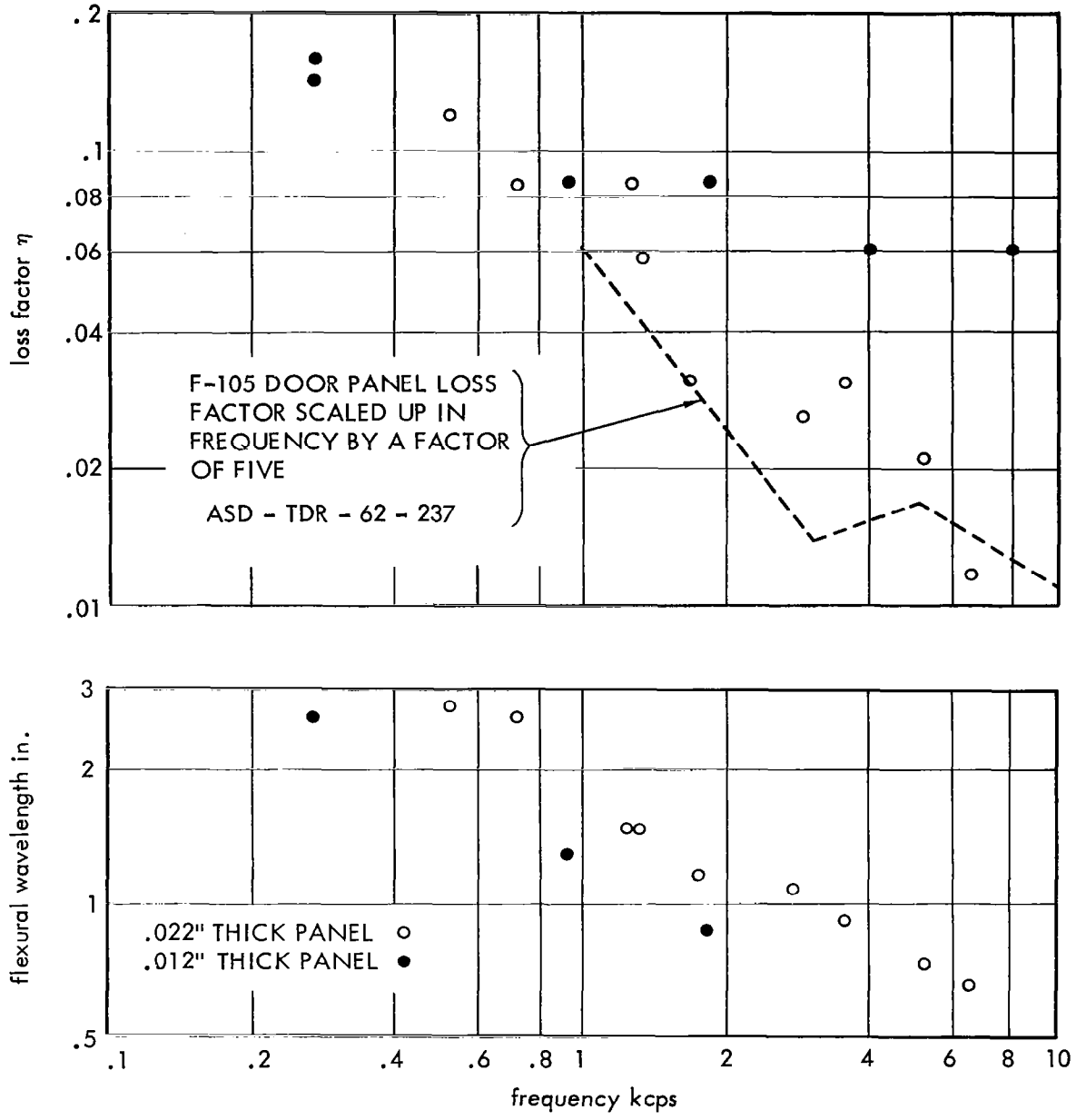

FIGURE 4. LOSS FACTOR η AND FLEXURAL WAVELENGTH AS A FUNCTION OF FREQUENCY FOR TWO TEST PANELS

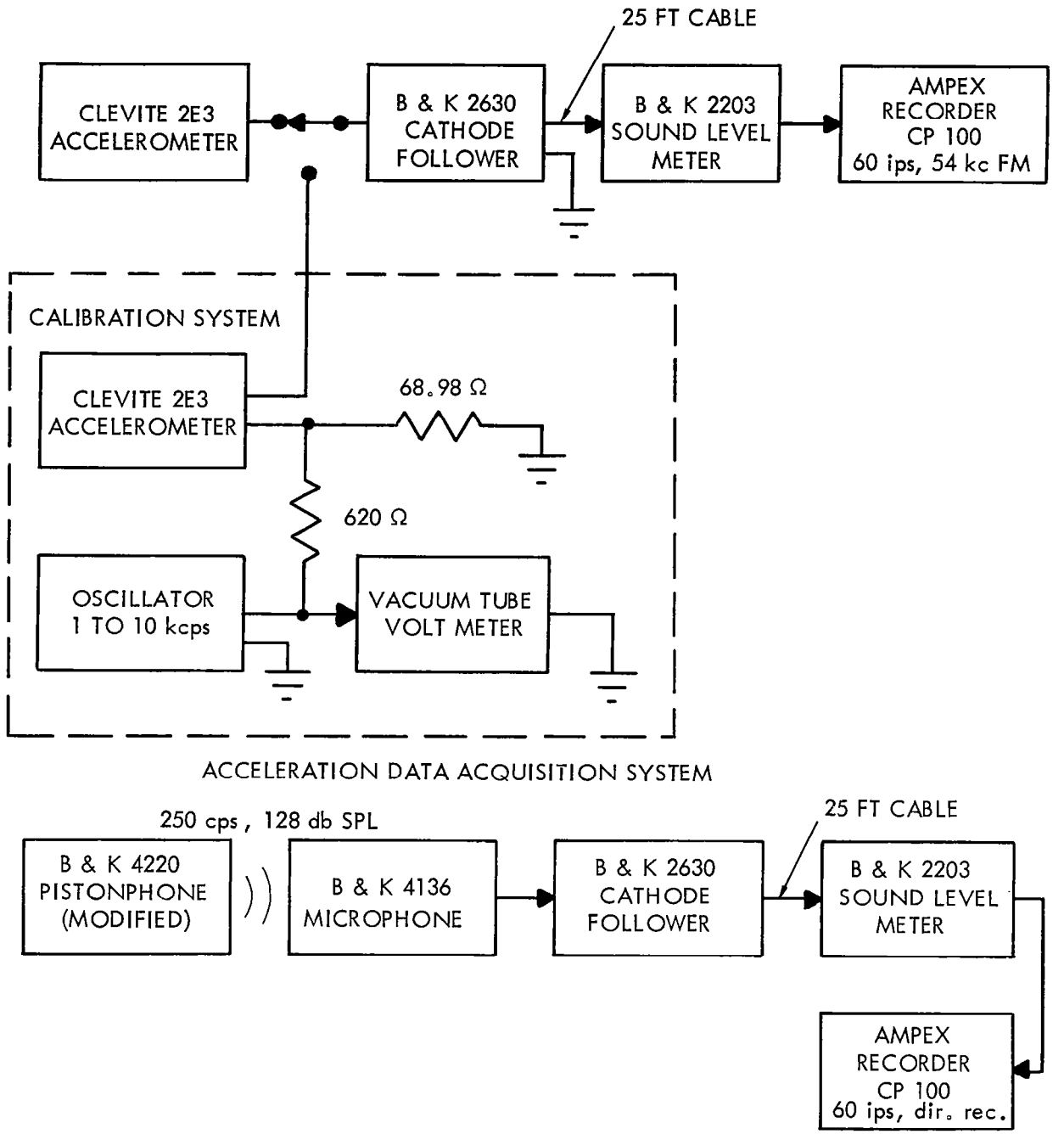

FIGURE 5. WIND TUNNEL TEST DATA ACQUISITION SYSTEMS

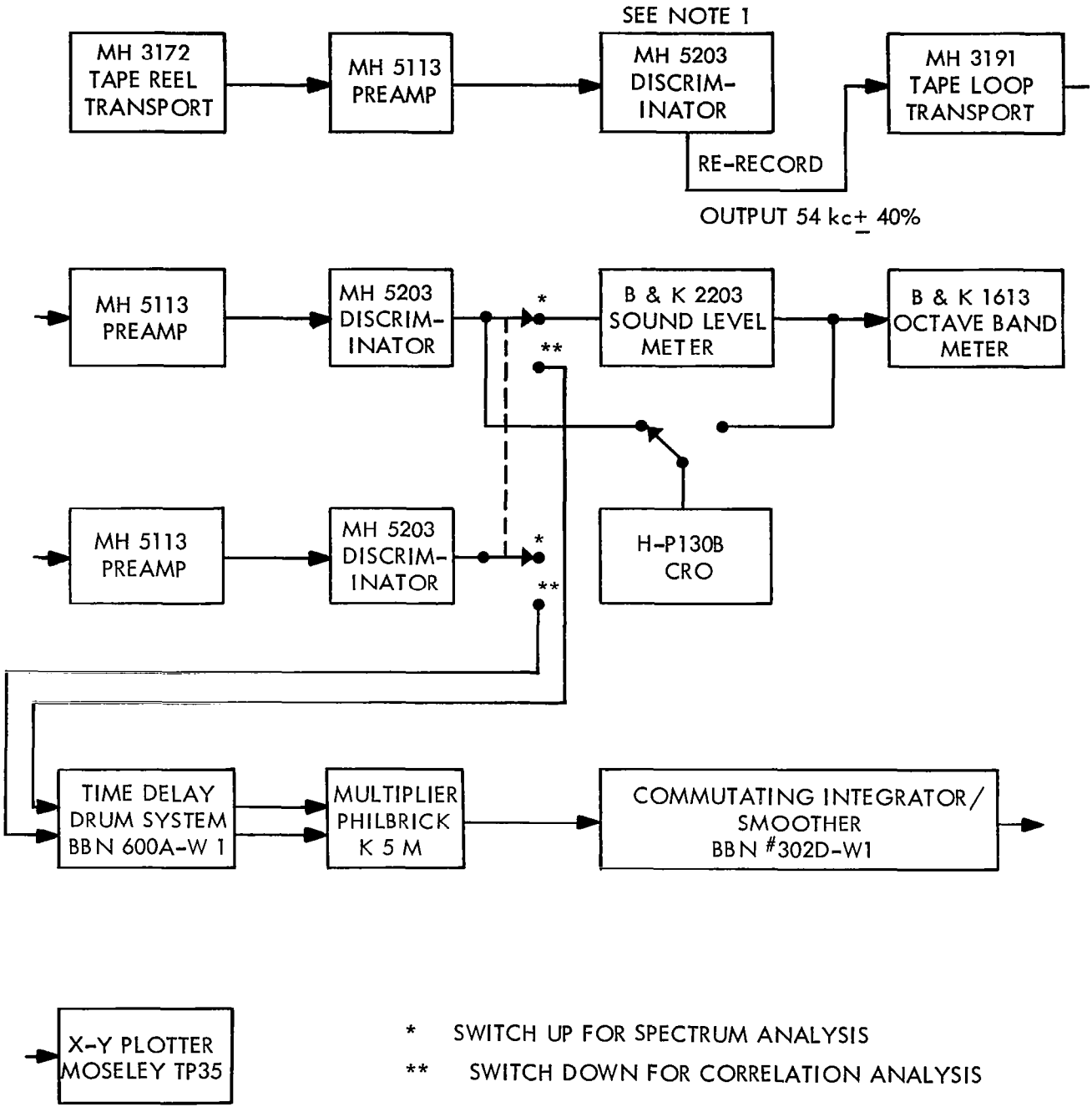

* SWITCH UP FOR SPECTRUM ANALYSIS

** SWITCH DOWN FOR CORRELATION ANALYSIS

NOTE 1: RE-RECORD OUTPUT IS NOT DISCRIMINATED BUT IS MERELY AMPLIFIED

FIGURE 6. WIND TUNNEL TEST DATA REDUCTION SYSTEMS

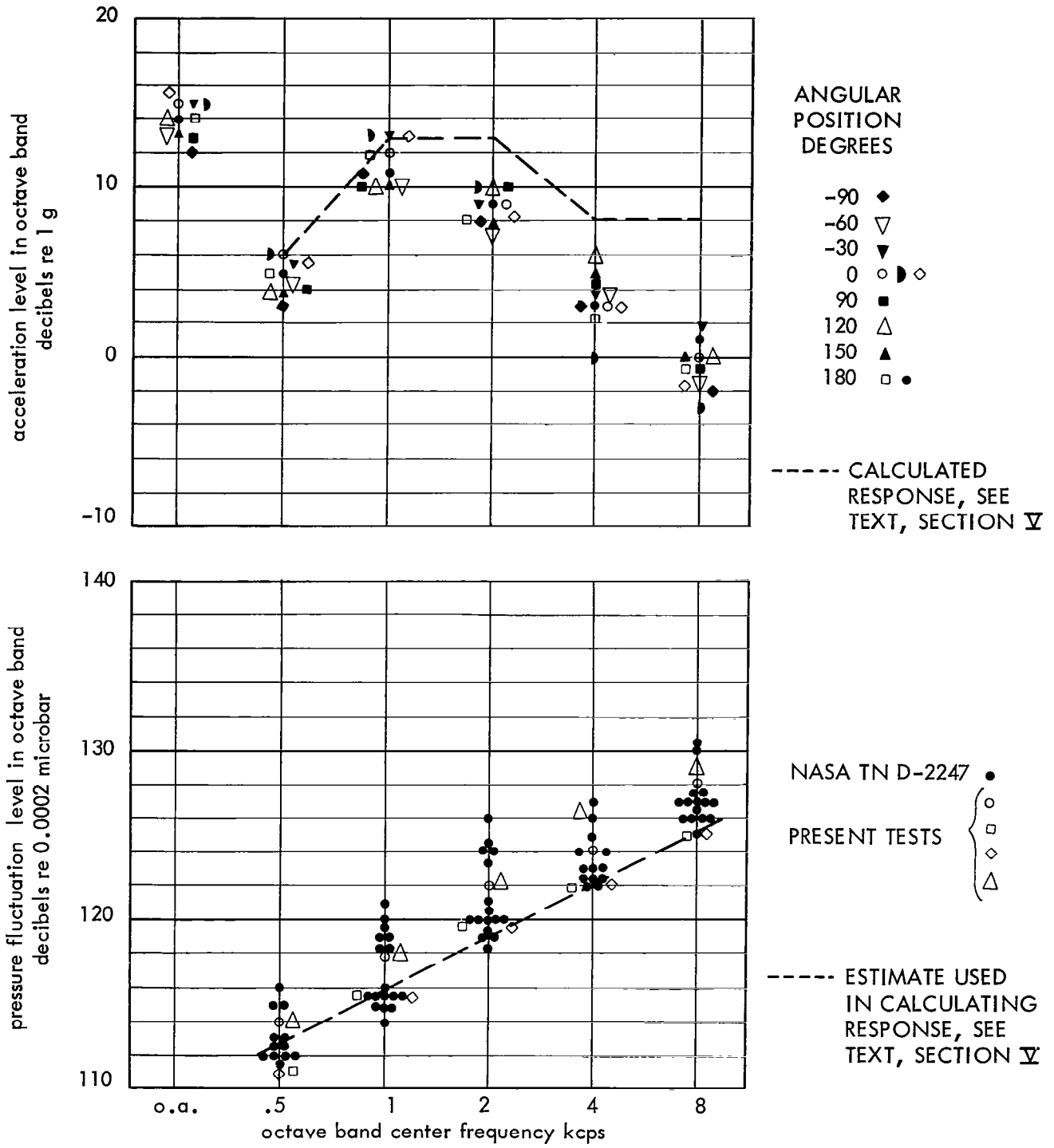

FIGURE 7a PANEL ACCELERATION LEVELS AND BOUNDARY LAYER PRESSURE FLUCTUATION LEVELS
.012" Thick Panel, Mach 3.5, Unperturbed Flow

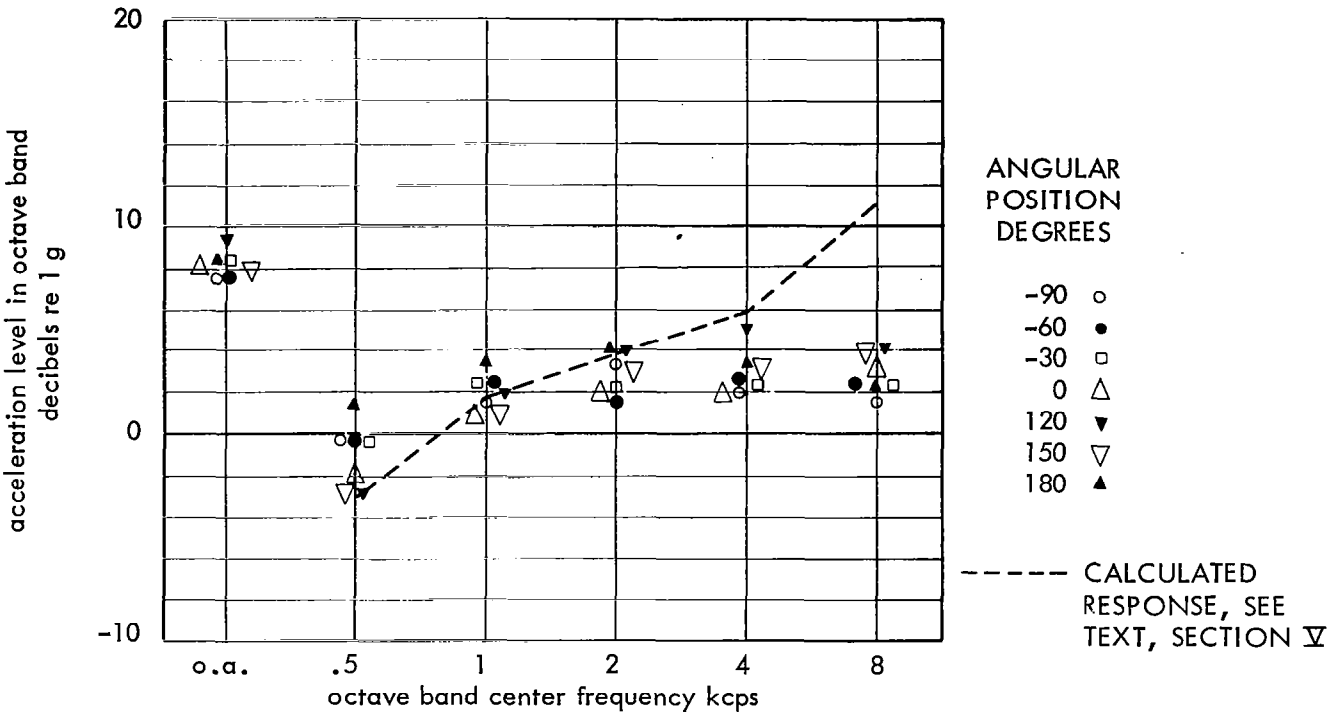

FIGURE 7b PANEL ACCELERATION LEVELS
.022" Thick Panel, Mach 3.5, Unperturbed Flow
(Boundary Layer Pressure Fluctuation Levels Shown in Part a of Figure)

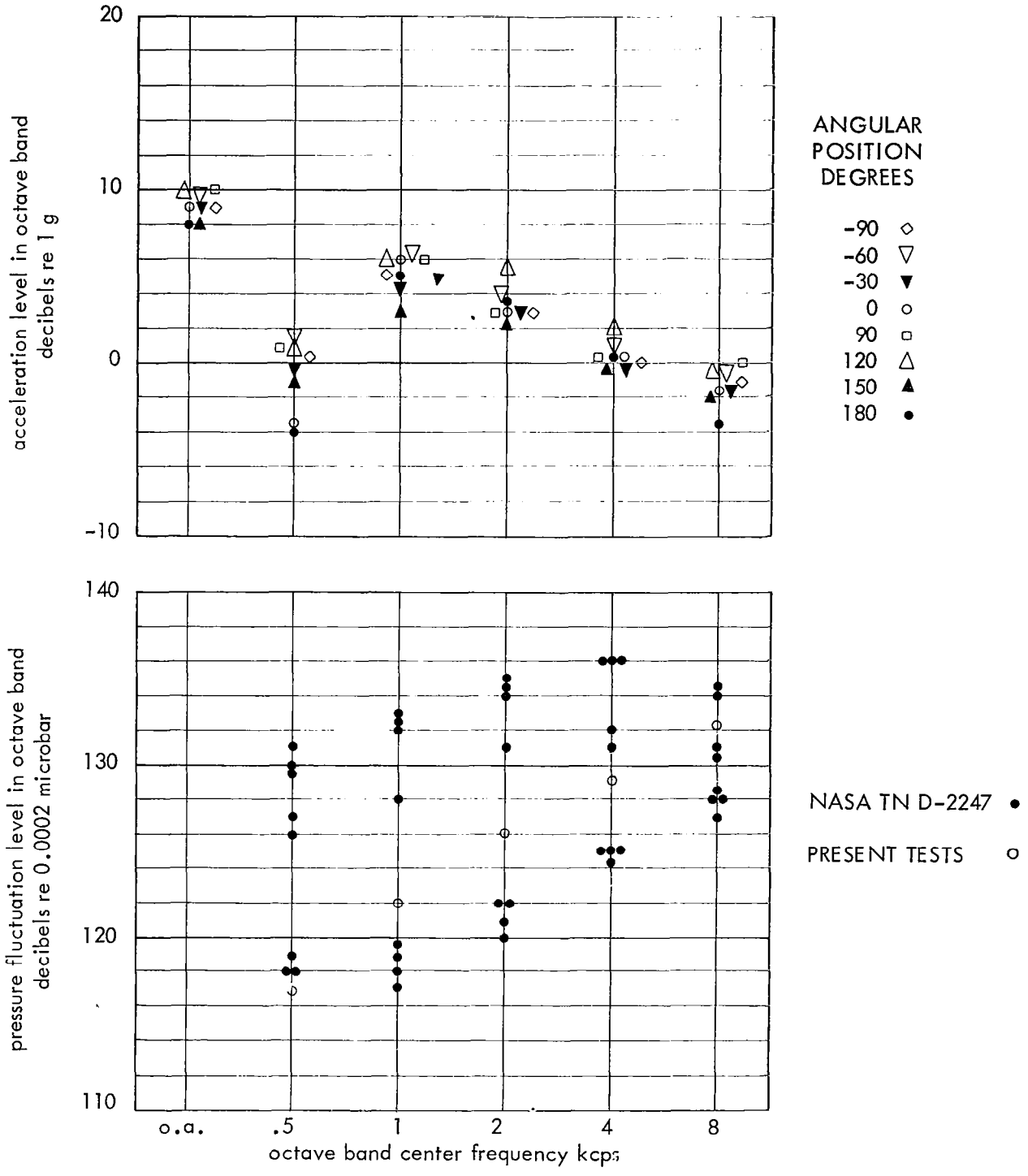

FIGURE 8a PANEL ACCELERATION LEVELS AND BOUNDARY LAYER PRESSURE FLUCTUATION LEVELS
.012" Thick Panel, Mach 1.4, Unperturbed Flow

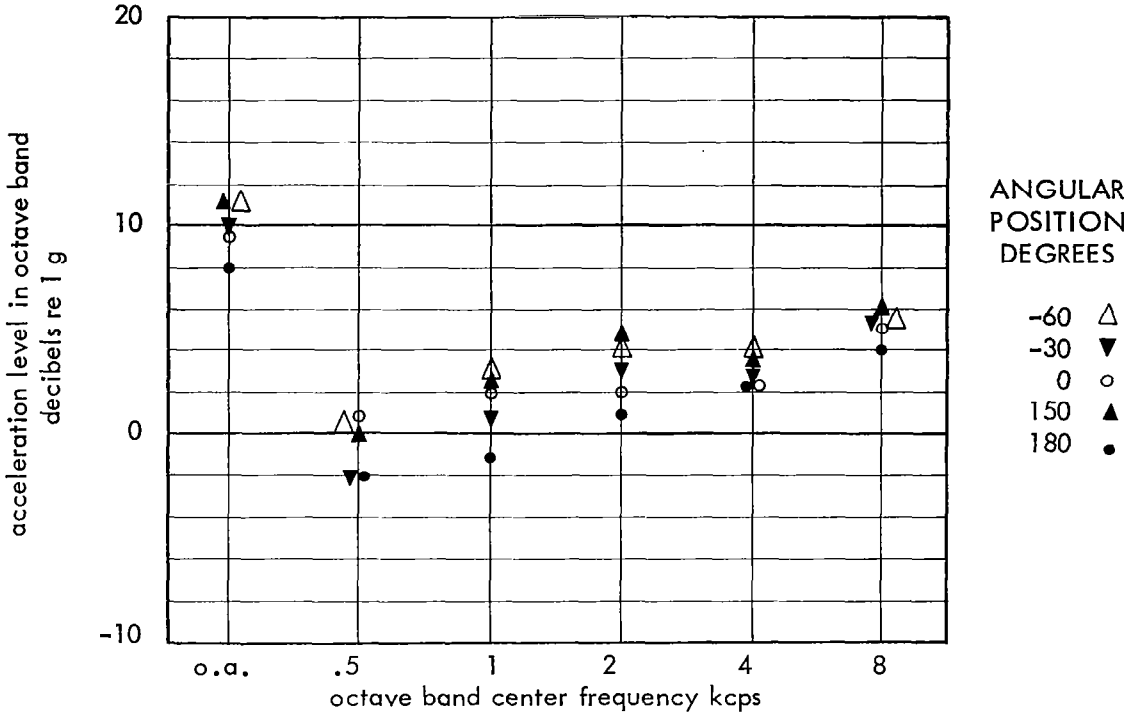

FIGURE 8b PANEL ACCELERATION LEVELS
.022" Thick Panel, Mach 1.4, Unperturbed Flow
(Boundary Layer Pressure Fluctuation Levels Shown in Part a of Figure)

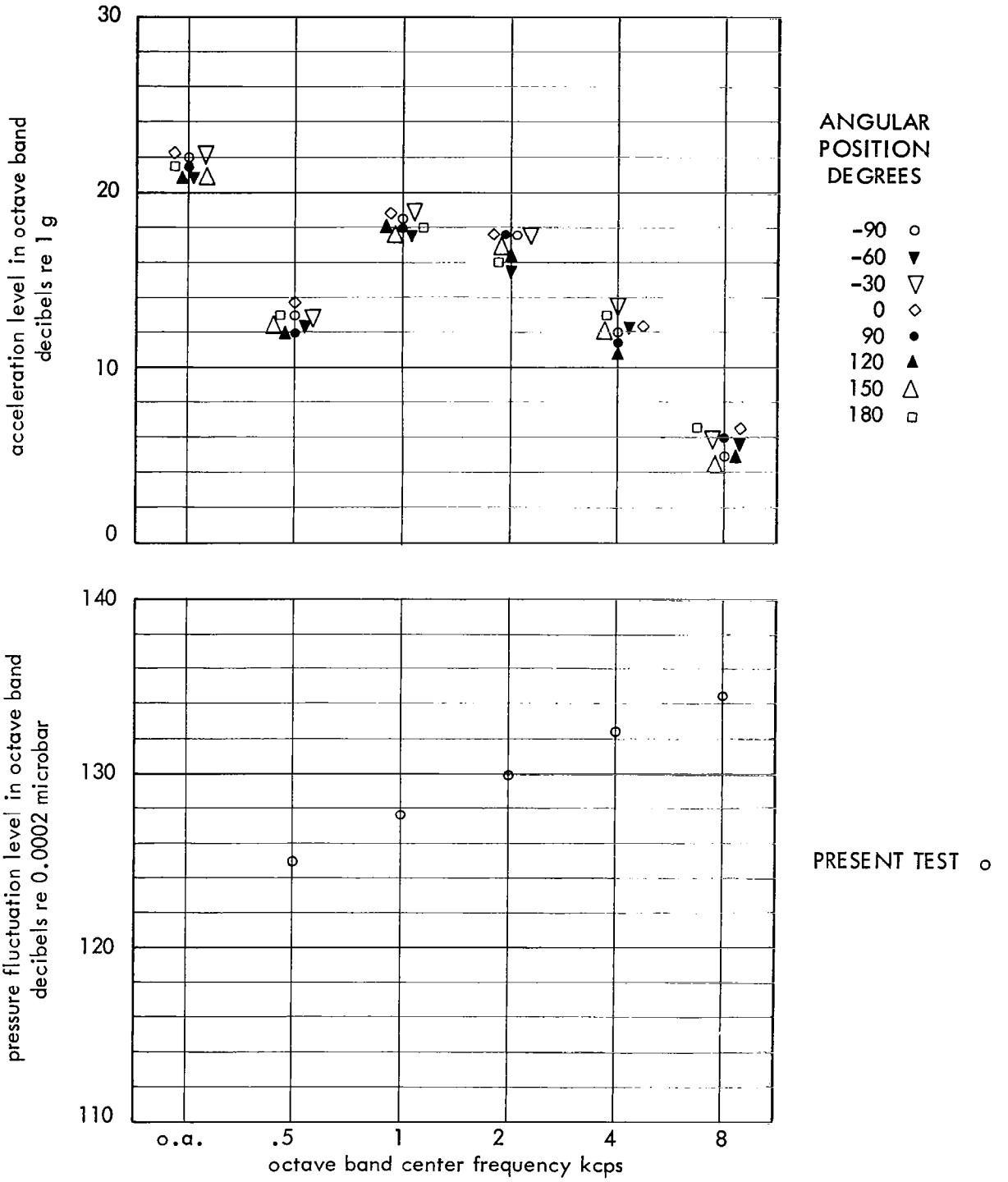

FIGURE 9. PANEL ACCELERATION LEVELS AND BOUNDARY LAYER PRESSURE FLUCTUATION LEVELS
.012" Thick Panel, Mach 3.5, Thickened Boundary Layer

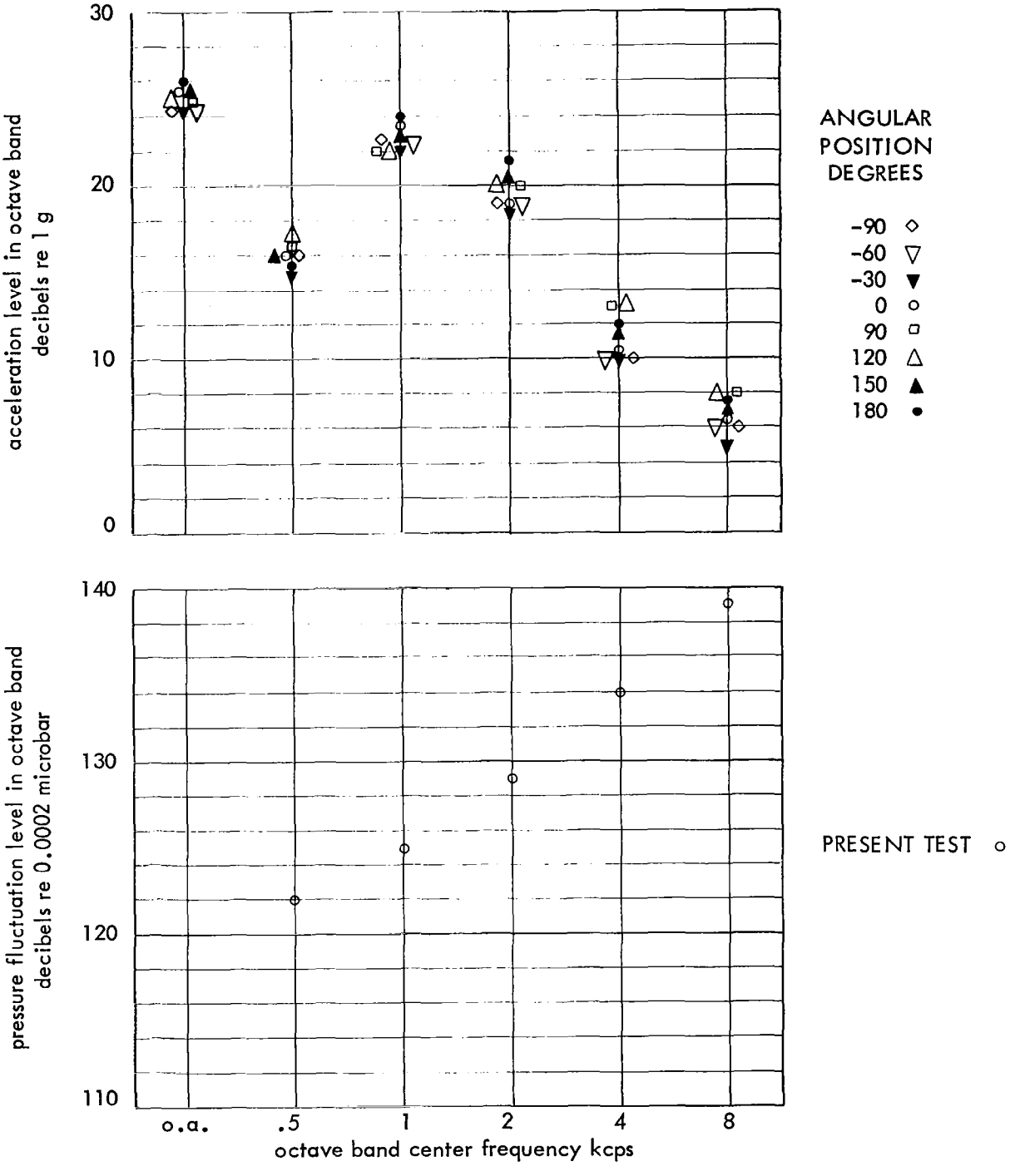

FIGURE 10a PANEL ACCELERATION LEVELS AND BOUNDARY LAYER PRESSURE FLUCTUATION LEVELS
.012" Thick Panel, Mach 3.5, Aft Facing 3/4" Step

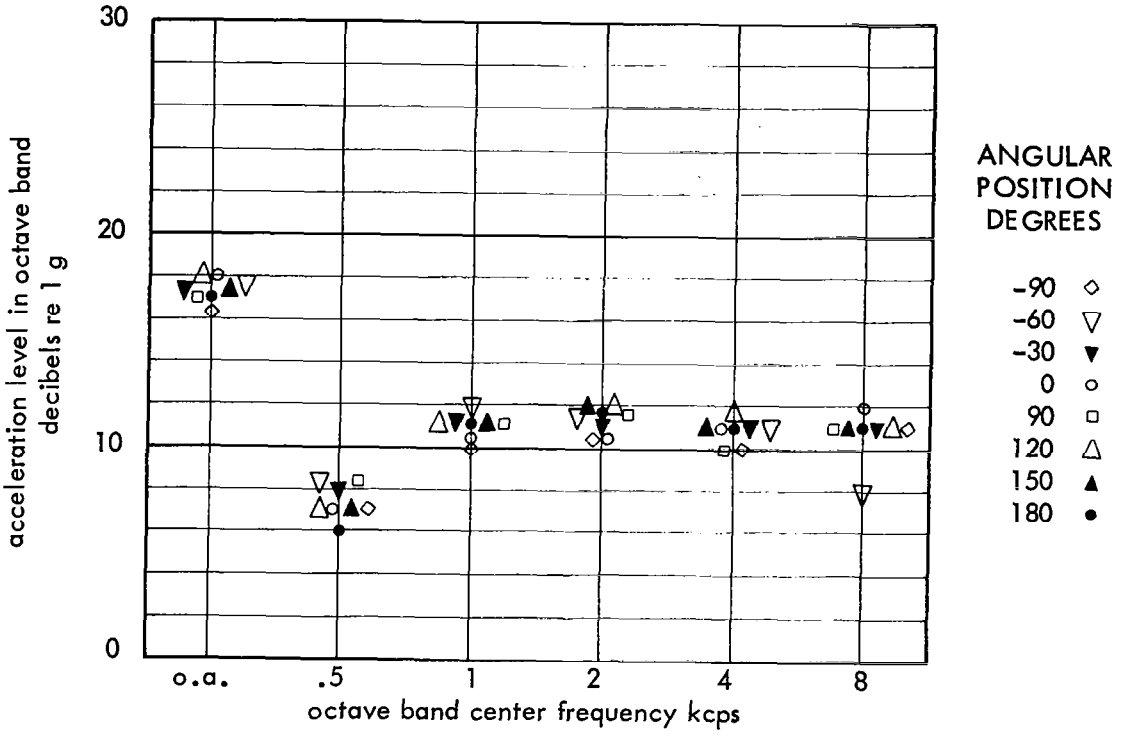

FIGURE 10b PANEL ACCELERATION LEVELS
.022" Thick Panel, Mach 3.5, Aft Facing 3/4" Step
(Boundary Layer Pressure Fluctuation Levels Shown in Part a of Figure)

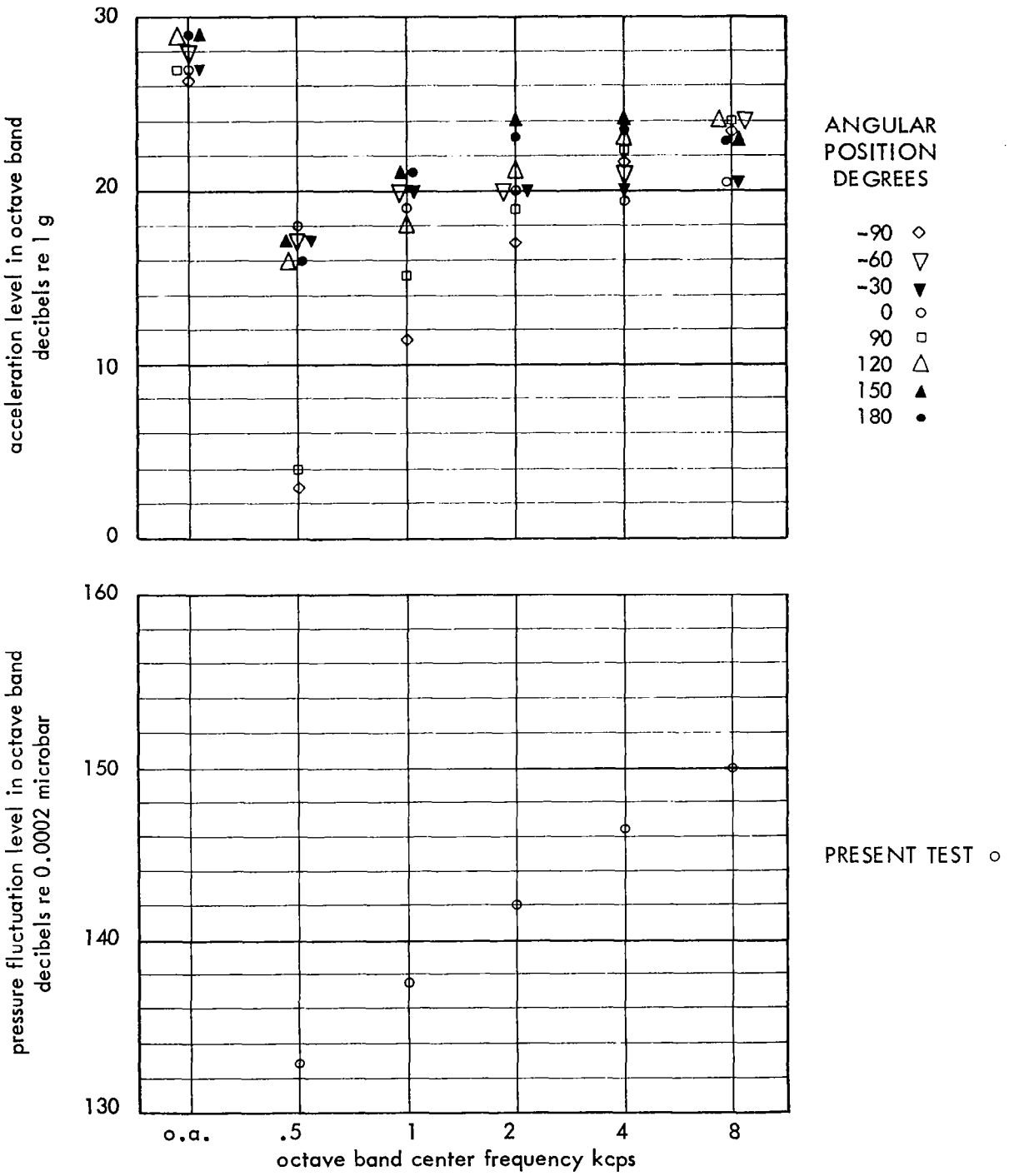

FIGURE 11. PANEL ACCELERATION LEVELS AND BOUNDARY LAYER PRESSURE FLUCTUATION LEVELS
.022" Thick Panel, Mach 1.4, Aft Facing 3/4" Step

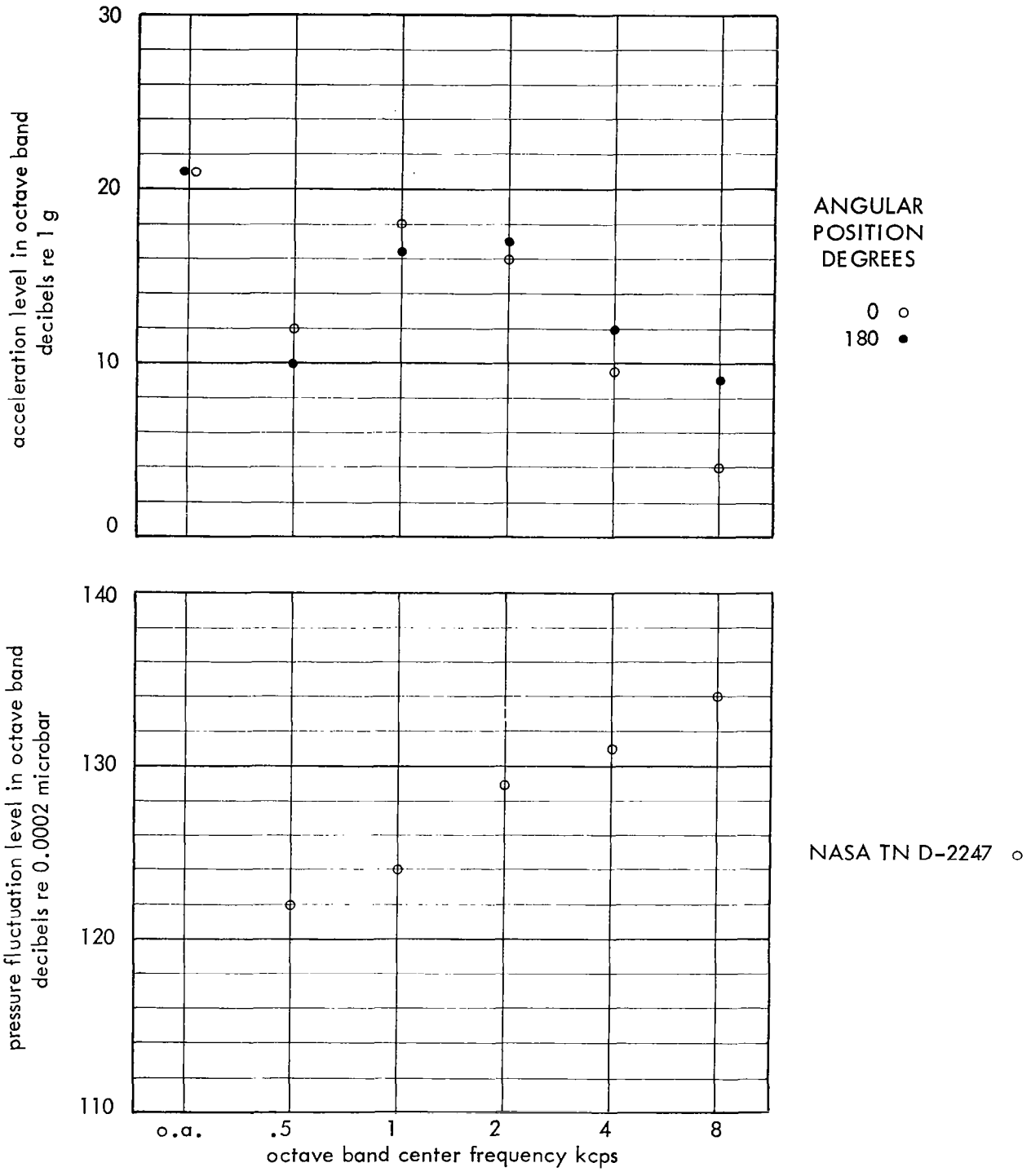

FIGURE 12a PANEL ACCELERATION LEVELS AND BOUNDARY LAYER PRESSURE FLUCTUATION LEVELS
.012" Thick Panel, Mach 3.5, Mild Shock

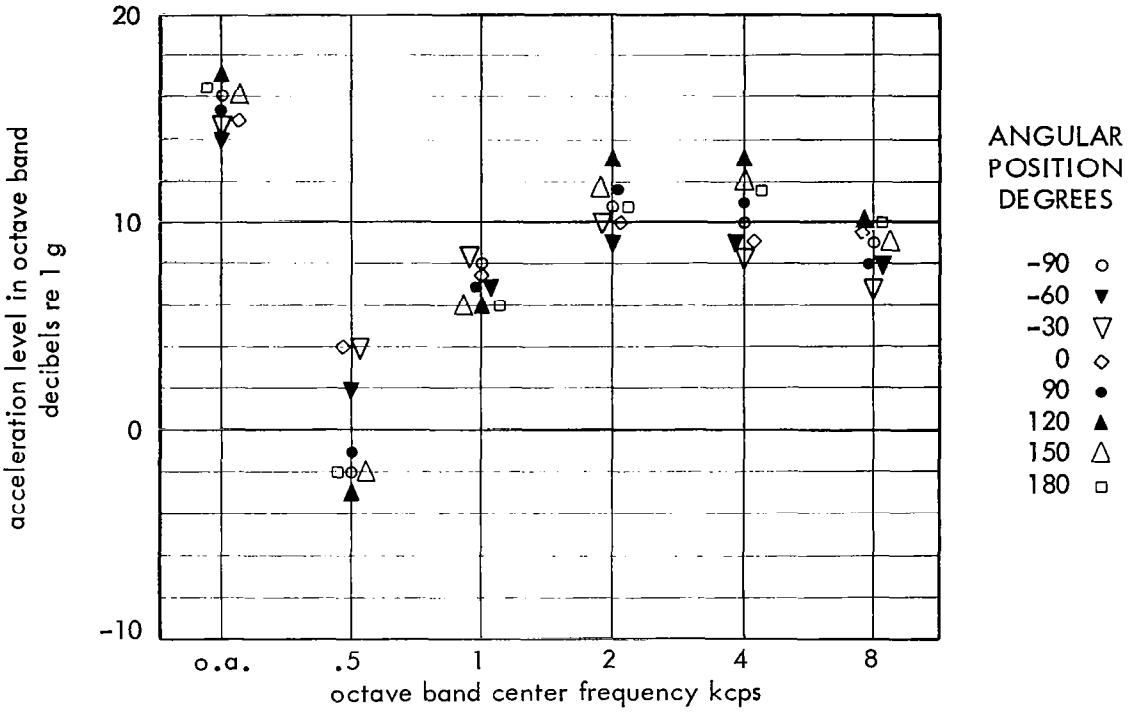

FIGURE 12b PANEL ACCELERATION LEVELS
.022" Thick Panel, Mach 3.5, Mild Shock
(Boundary Layer Pressure Fluctuation Levels Shown in Part a of Figure)

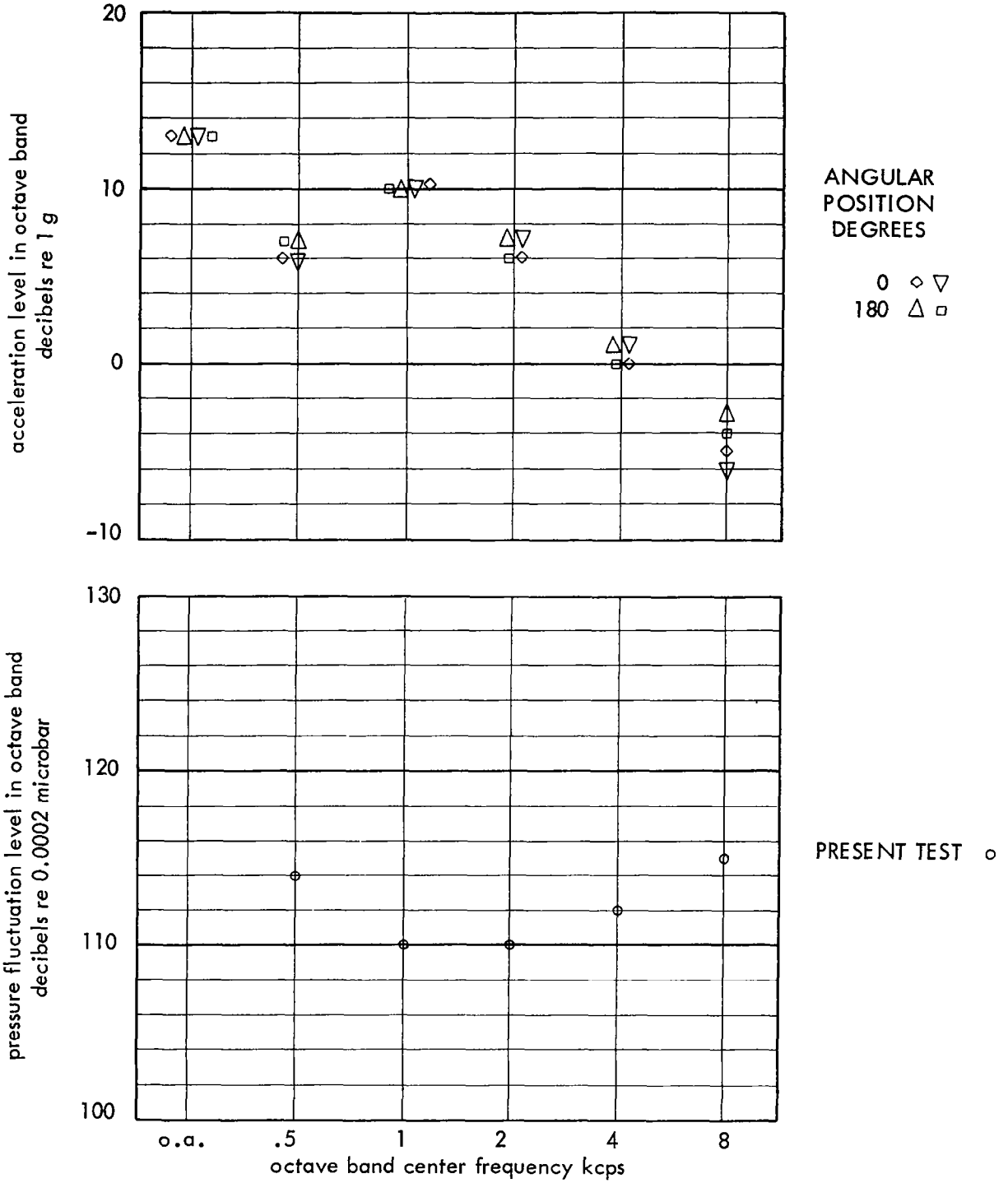

FIGURE 13a PANEL ACCELERATION LEVELS AND BOUNDARY LAYER PRESSURE FLUCTUATION LEVELS
.012" Thick Panel, Mach 3.5, Mild Expansion

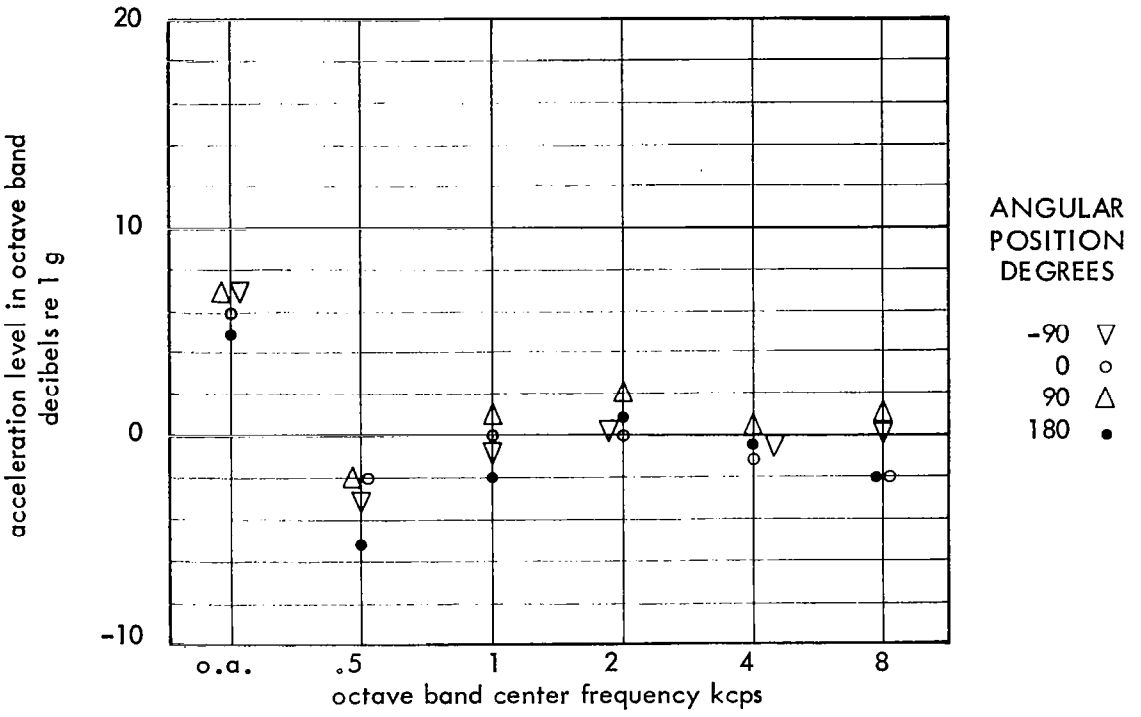

FIGURE 13b PANEL ACCELERATION LEVELS
.022" Thick Panel, Mach 3.5, Mild Expansion
(Boundary Layer Pressure Fluctuation Levels Shown in Part a of Figure)

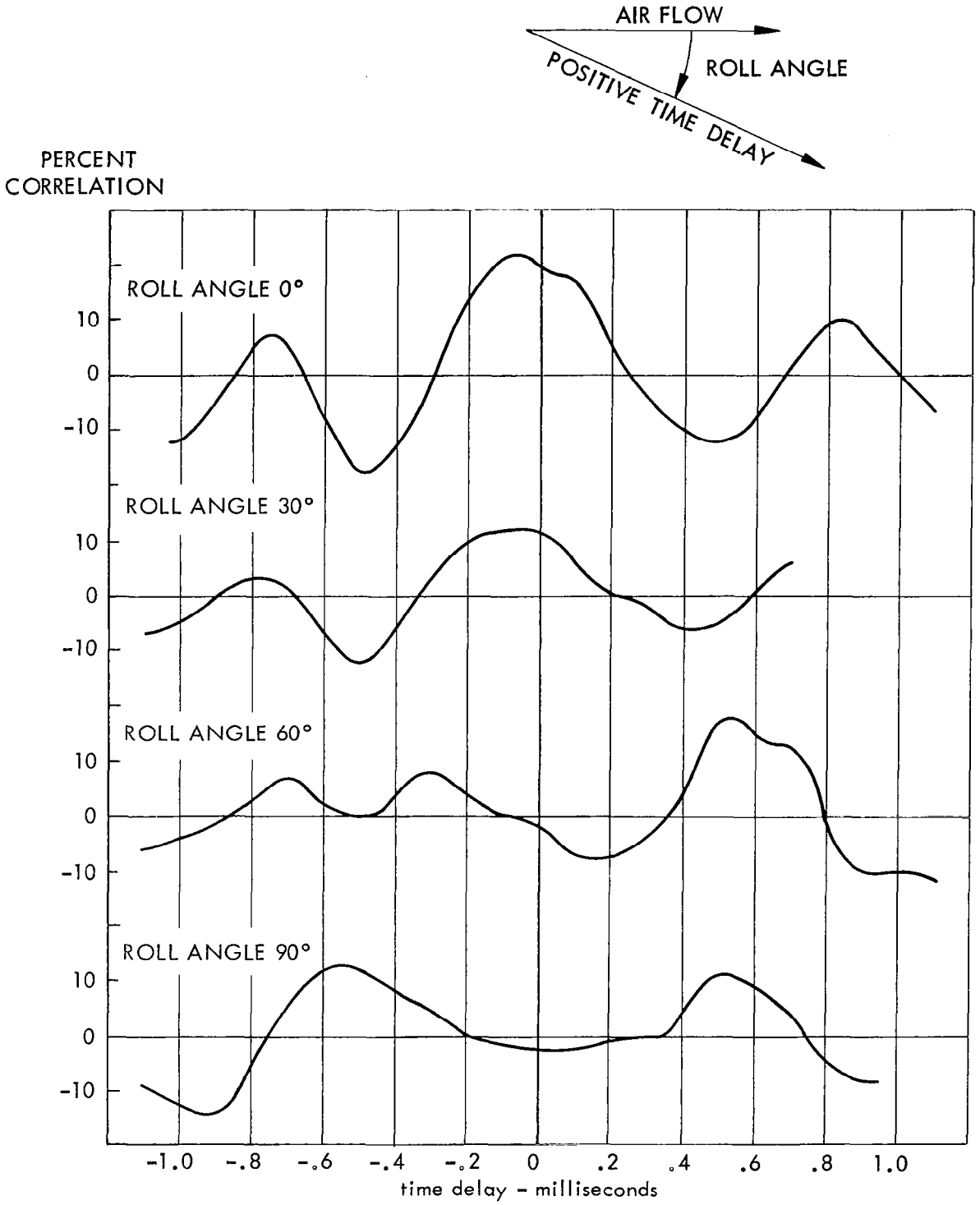

FIGURE 14. PANEL ACCELERATION CROSS CORRELATION
.012" Thick Panel, Mach 3.5, Unperturbed Flow
(For roll angles less than 90°, positive delay corresponds to disturbance propagation with a component in the direction of flow)

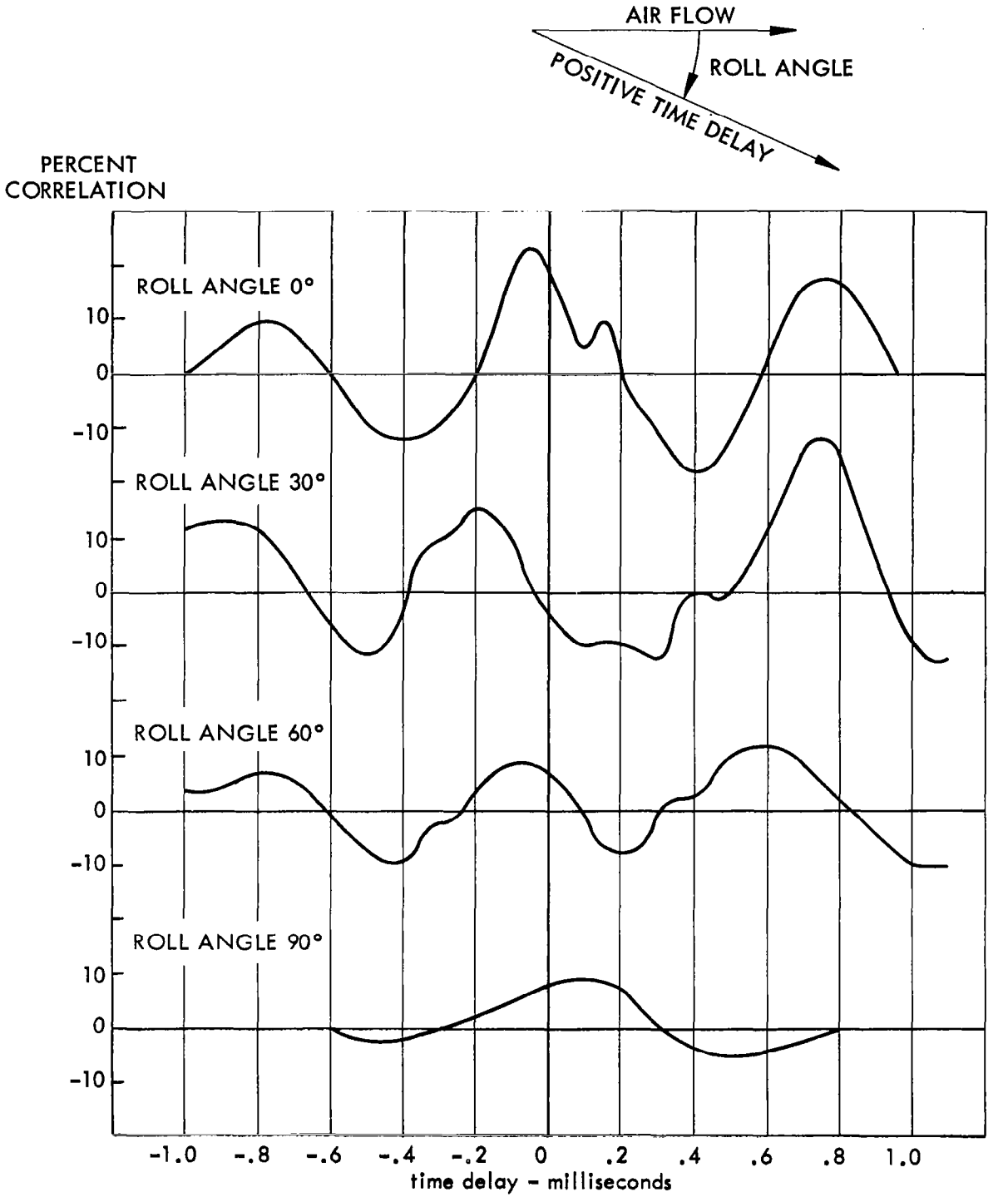

FIGURE 15. PANEL ACCELERATION CROSS CORRELATION
.012" Thick Panel, Mach 1.4, Unperturbed Flow
(For roll angles less than 90°, positive delay corresponds to disturbance propagation with a component in the direction of flow)

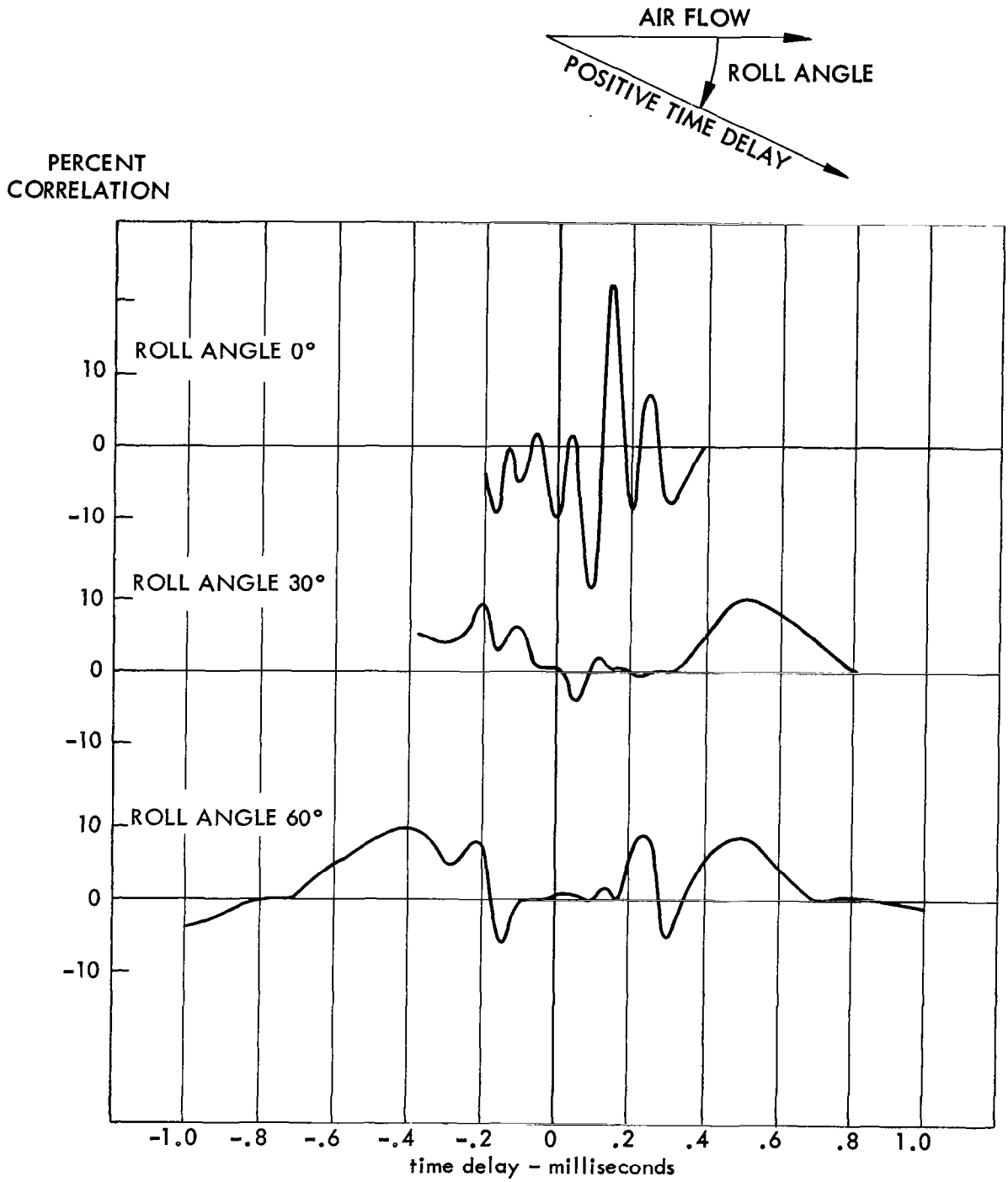

FIGURE 16. PANEL ACCELERATION CROSS CORRELATION
.022" Thick Panel, Mach 1.4, Unperturbed Flow
(Positive delay corresponds to disturbance propagation with a component in the direction of flow)

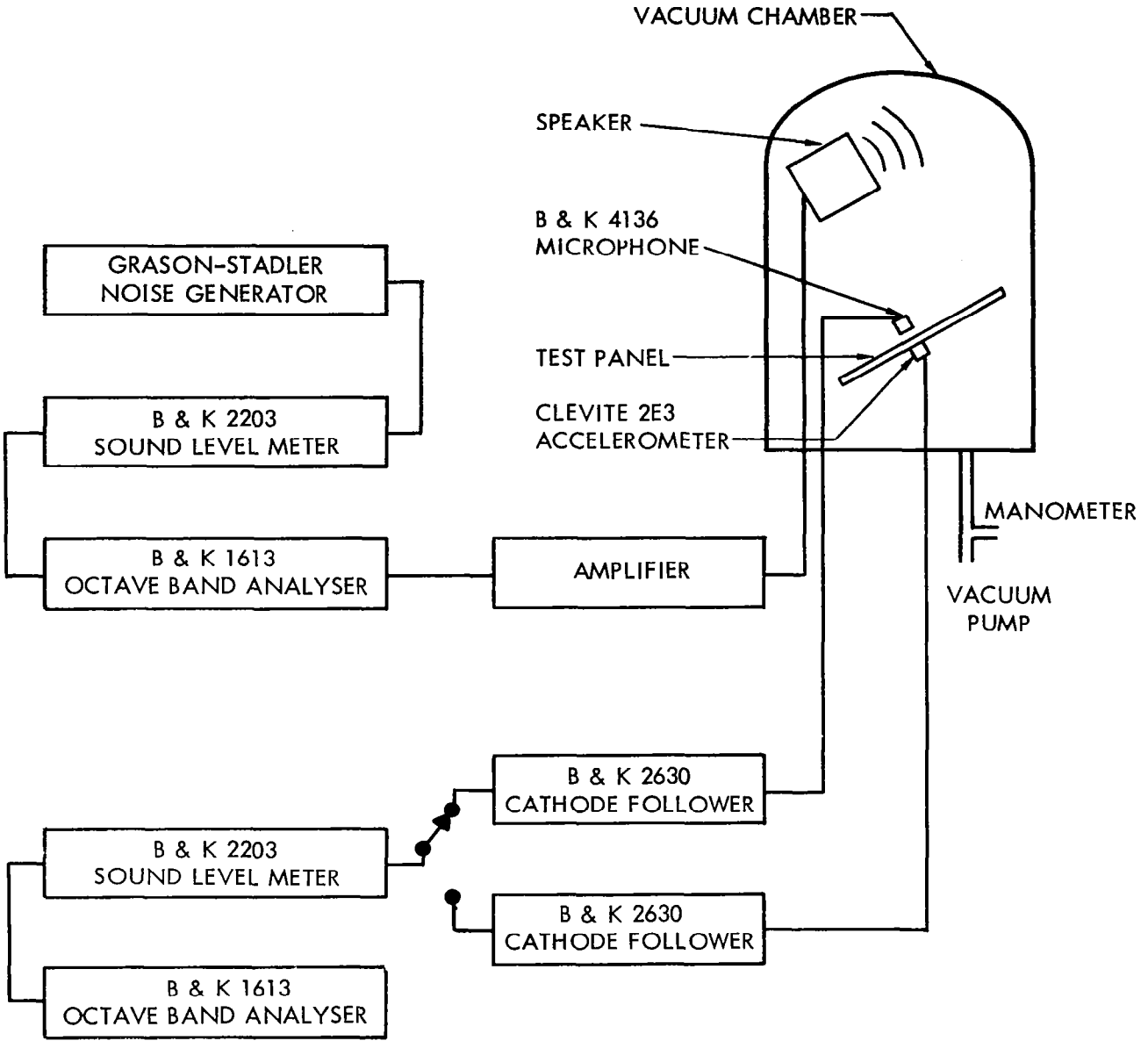

FIGURE 17. TEST APPARATUS FOR DETERMINING RESPONSE OF TEST PANEL TO REVERBERANT ACOUSTIC FIELD AT VARIOUS STATIC PRESSURE

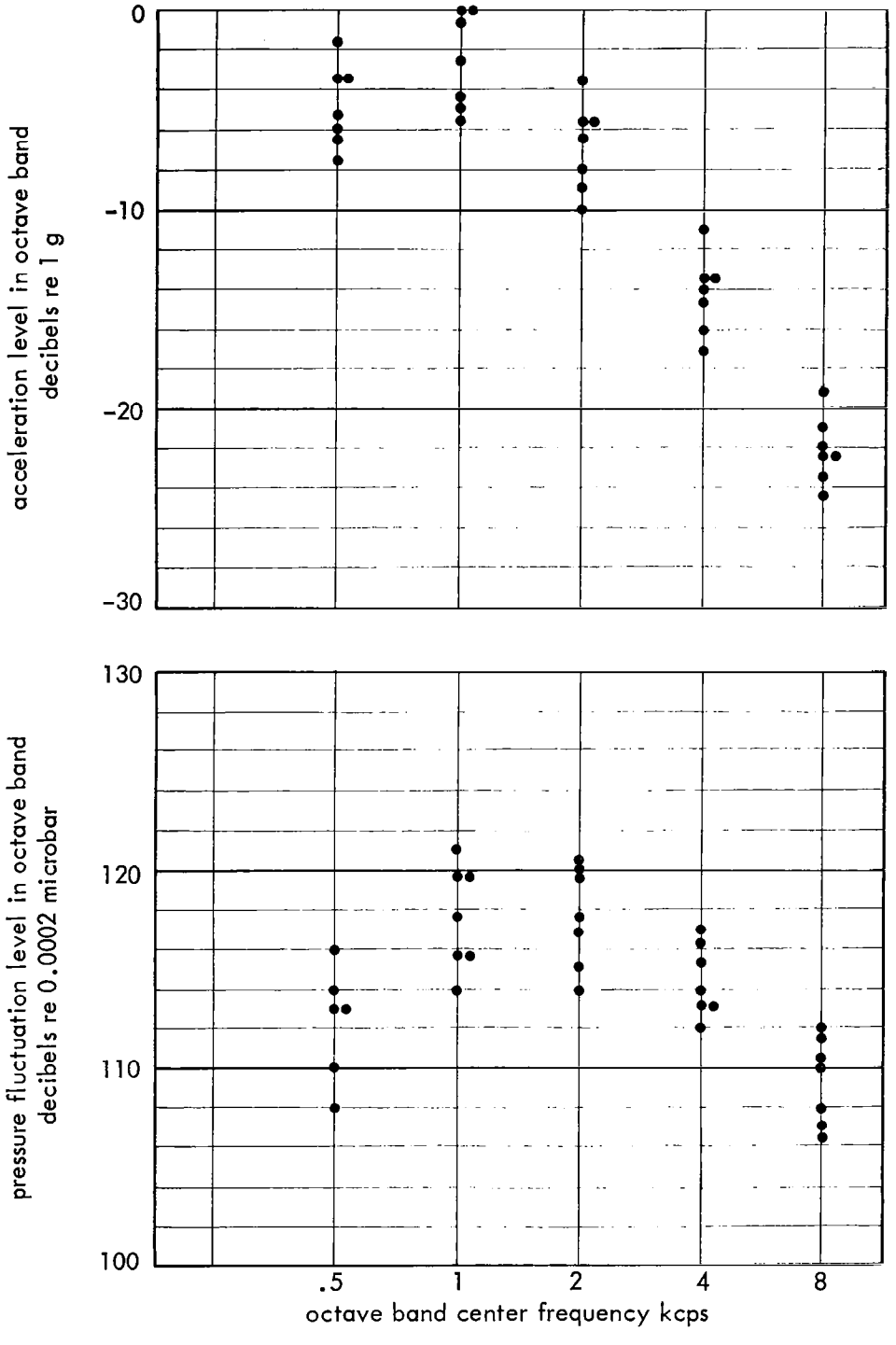

FIGURE 18. TYPICAL ACOUSTIC TEST DATA SHOWING PANEL ACCELERATION LEVELS AND SOUND PRESSURE LEVELS
.012" Thick Panel with Backing Plate Removed, Static Pressure 7 psia

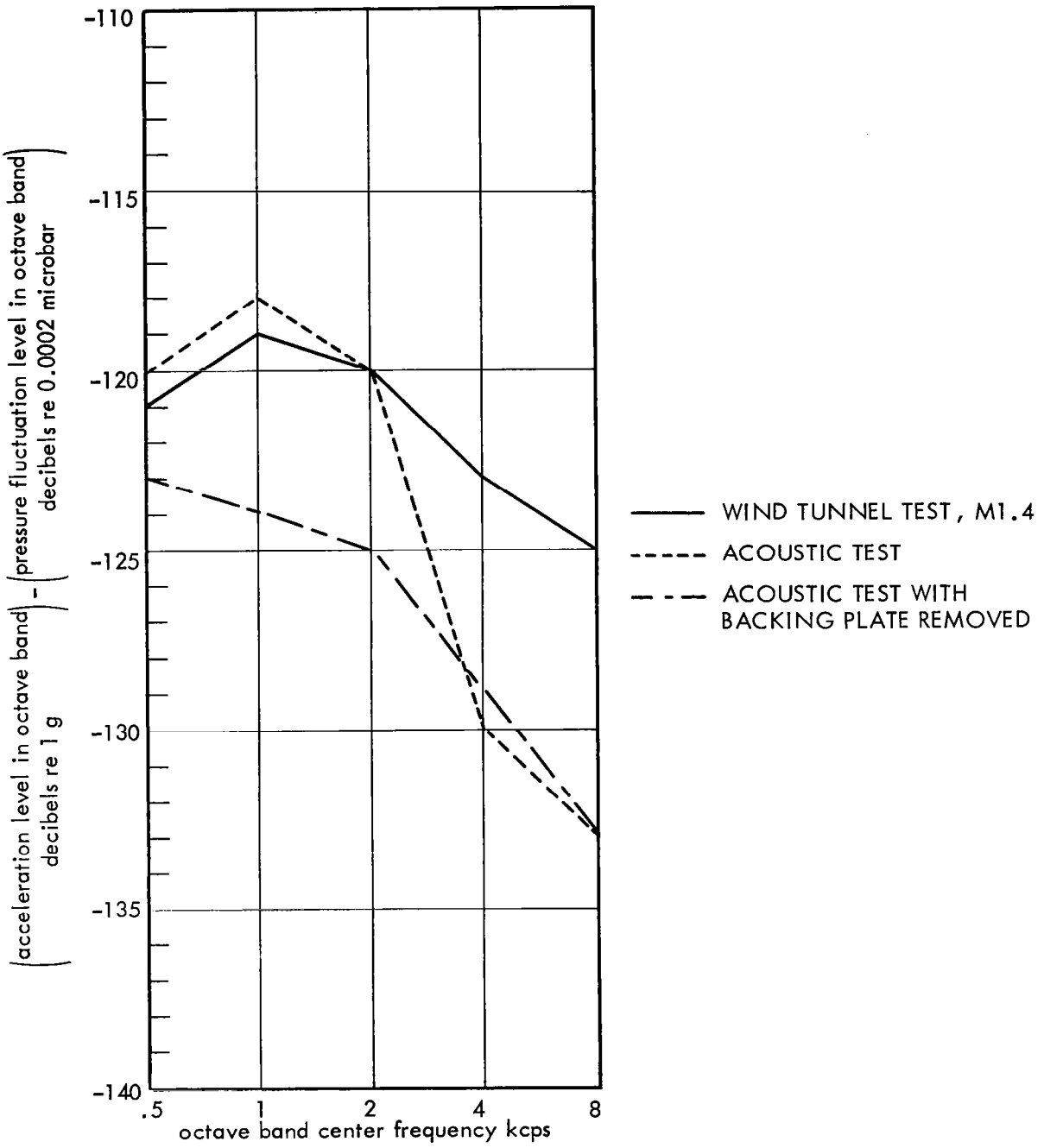

FIGURE 19. PRESSURE-FLUCTUATION-TO-ACCELERATION TRANSFER FUNCTION FOR WIND TUNNEL AND ACOUSTIC TESTS
.022" Thick Panel, Static Pressure 7 psia

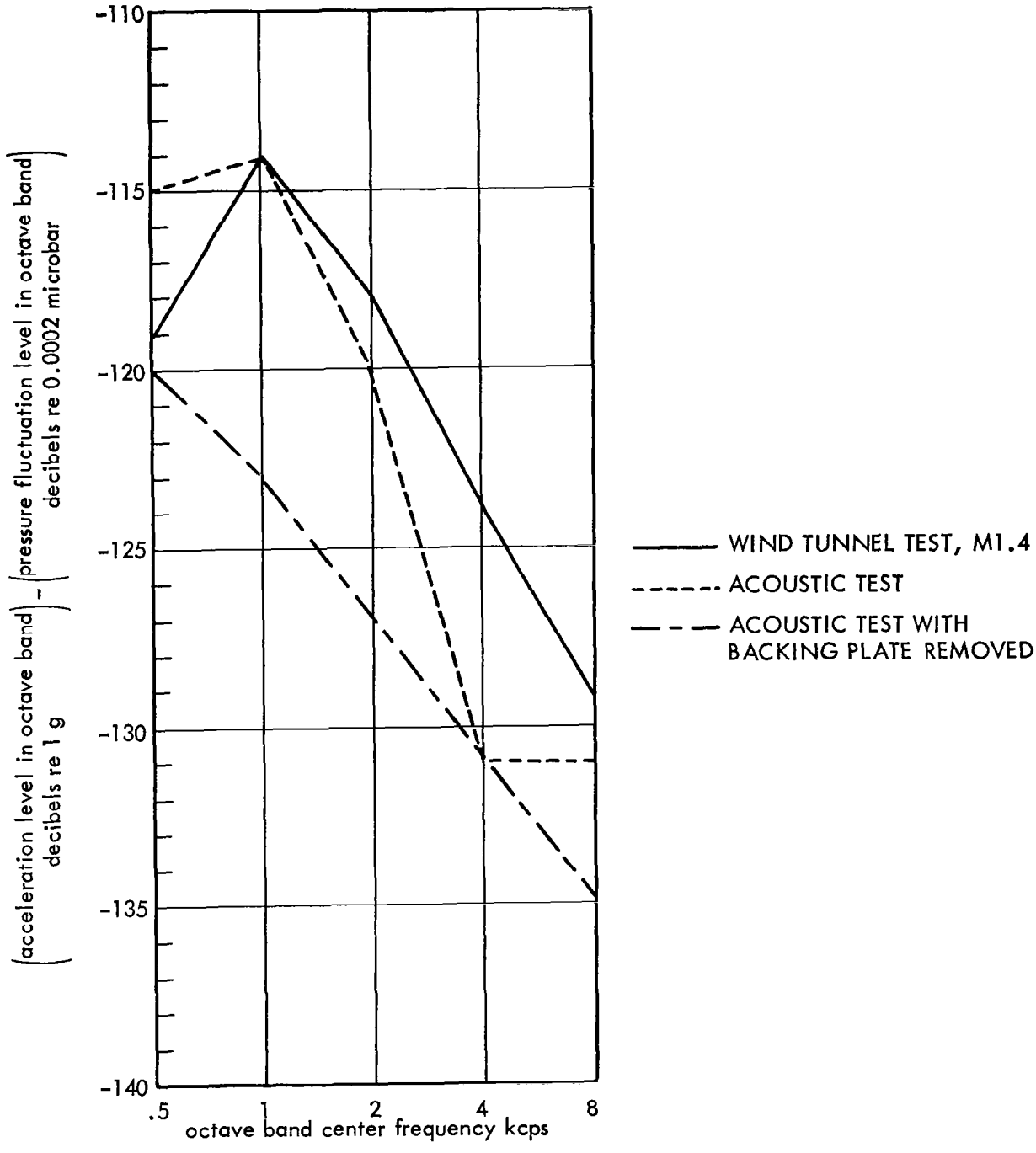

FIGURE 20. PRESSURE-FLUCTUATION-TO-ACCELERATION TRANSFER FUNCTIONS FOR WIND TUNNEL AND ACOUSTIC TESTS
.012" Thick Panel, Static Pressure 7 psia

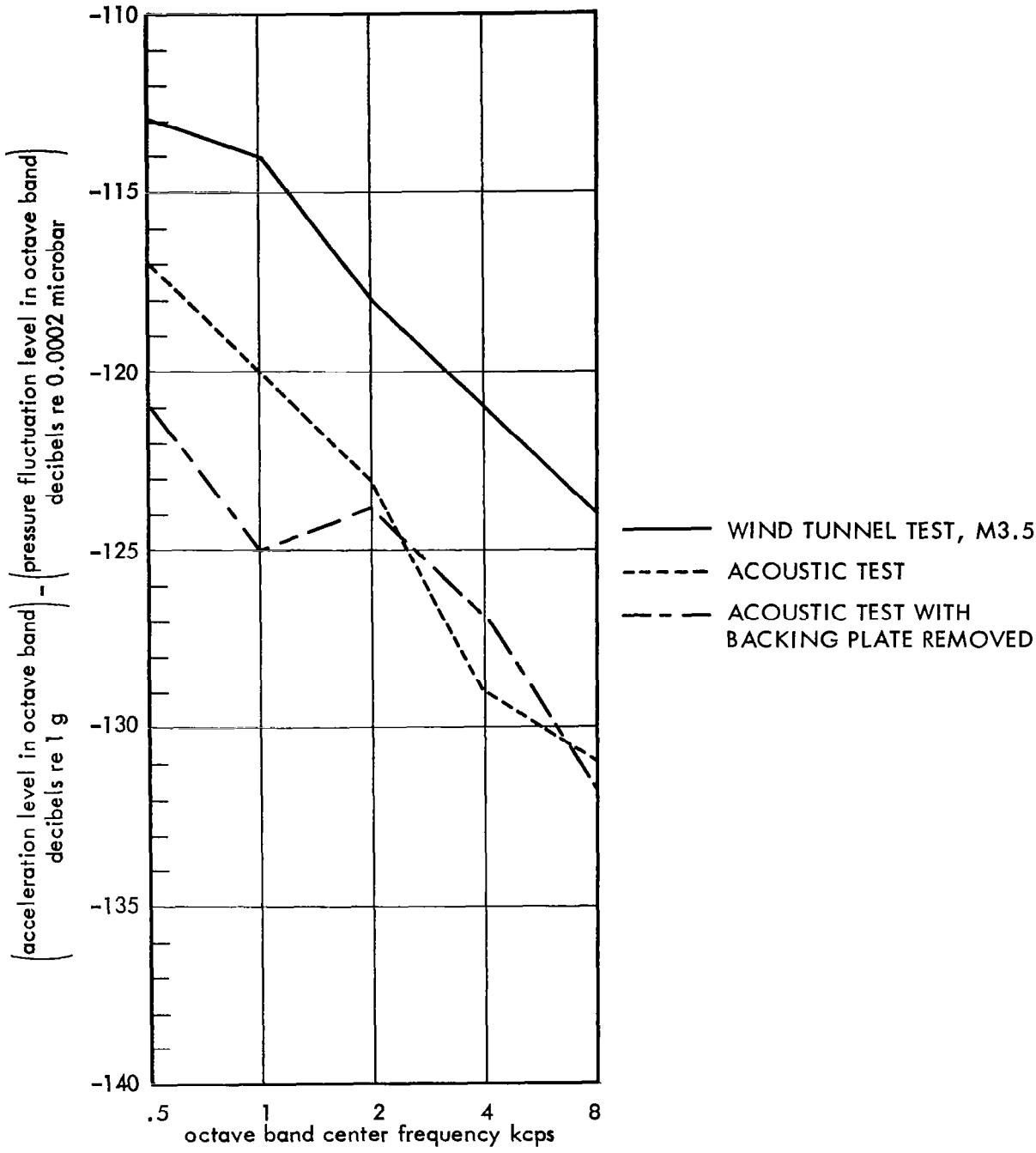

FIGURE 21. PRESSURE-FLUCTUATION-TO-ACCELERATION TRANSFER FUNCTIONS FOR WIND TUNNEL AND ACOUSTIC TESTS
.022" Thick Panel, Static Pressure 1.5 psia

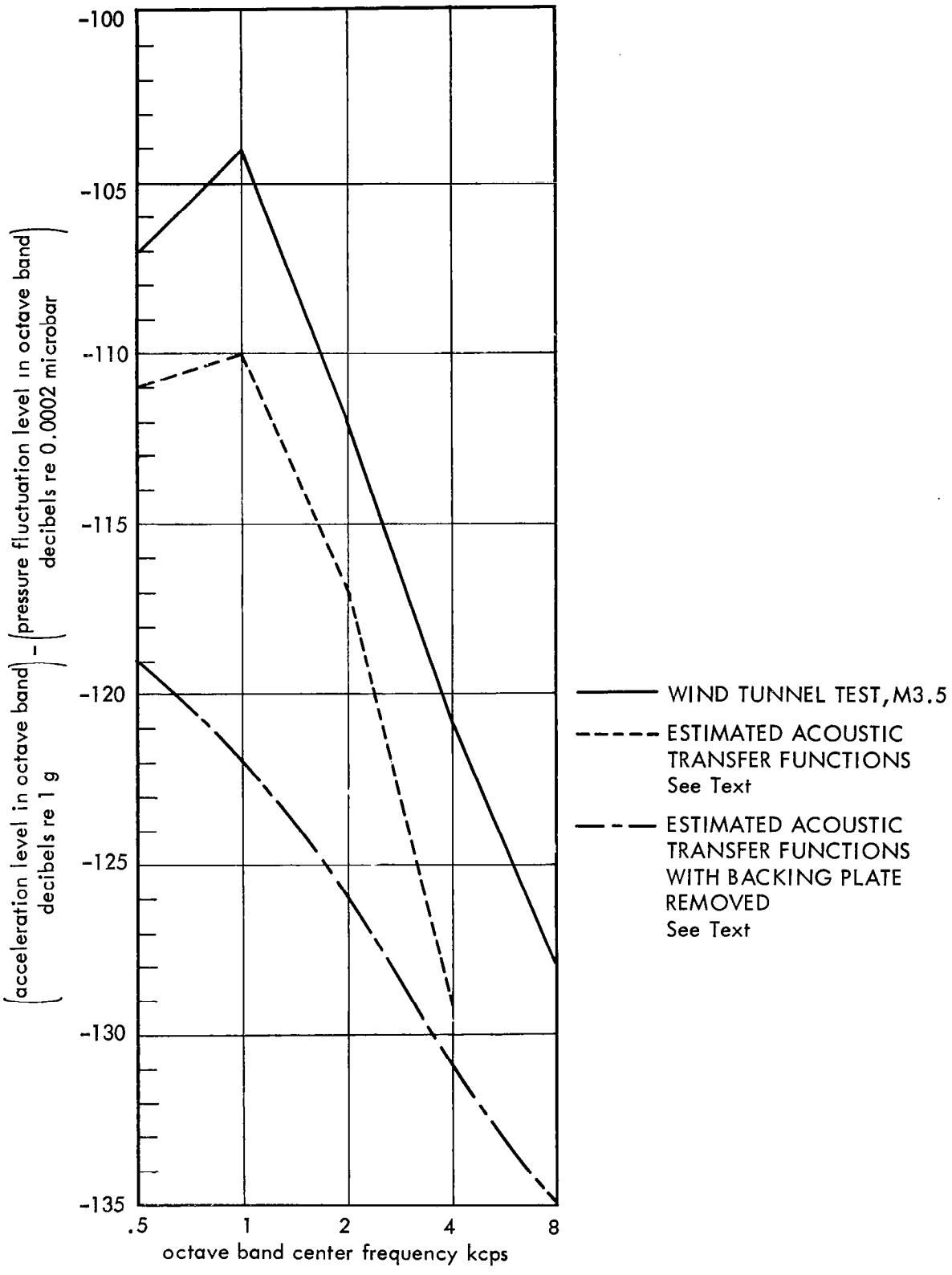

FIGURE 22. PRESSURE-FLUCTUATION-TO-ACCELERATION TRANSFER FUNCTIONS FOR WIND TUNNEL AND ACOUSTIC TESTS
.012" Thick Panel, Static Pressure 1.5 psi

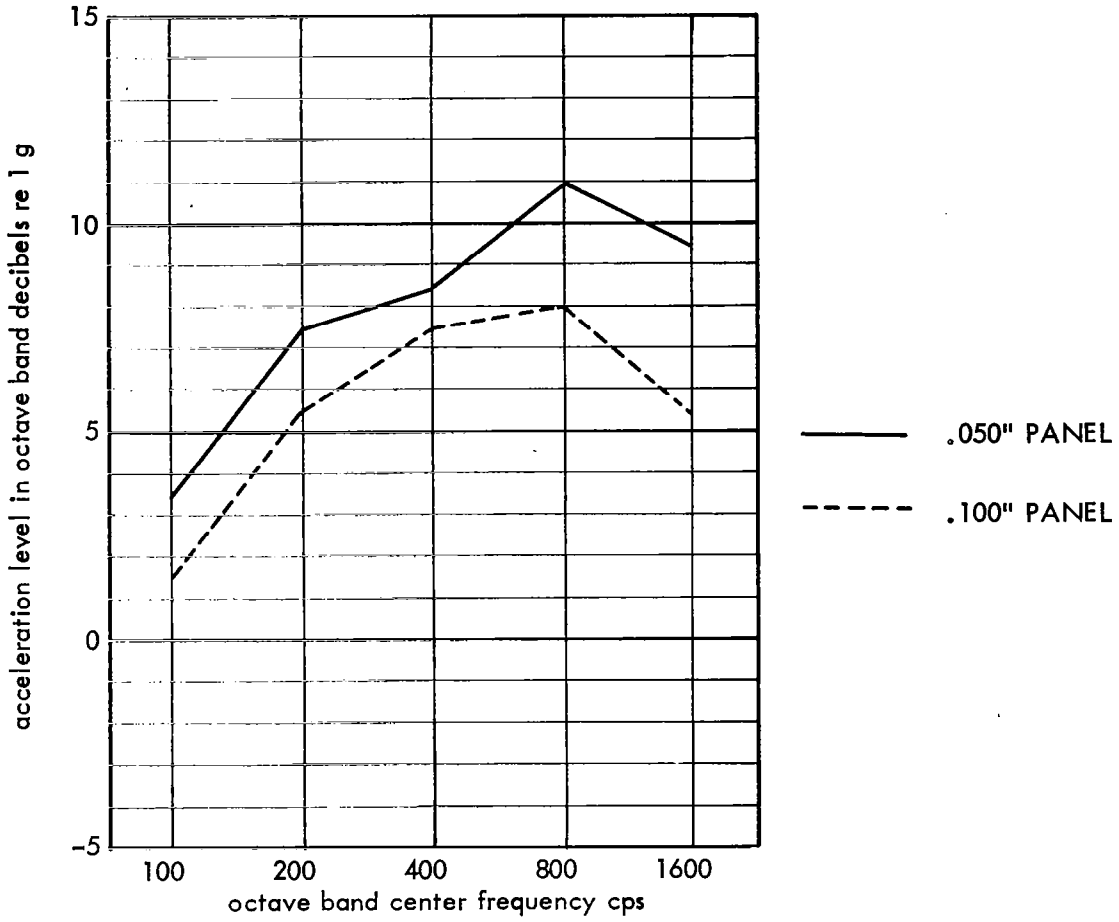

FIGURE 23. EXPECTED RESPONSE OF TWO PANELS AT MACH 3.5 AT 70,000 FT ALTITUDE
Based on Model Tests Scaled By a Factor of Five and Corrected for Damping With an Assumed Flat Pressure Fluctuation Spectrum Level of 100 dB re 0.0002 Microbar
(See Appendix A and Test)